THE VORTEX INDUCED OSCILLATION OF ELASTIC STRUCTURAL ELEMENTS

Thesis by

Tadashi Shiraishi

In Partial Fulfillment of the Requirements

for the Degree of

Mechanical Engineer

California Institute of Technology

Pasadena, California

1977

(Submitted on February 25, 1977)

ACKNOWLEDGMENTS

The author wishes to express his gratitude to Dr. W. D. Iwan and Dr. A. J. Acosta for their guidance and encouragement during the course of his graduate studies and in the preparation of this work. He is pleased to acknowledge the valuable suggestions of Dr. A. Roshko and Dr. R. D. Blevins.

The author wishes to thank Miss Sharon Vedrode for her skillful typing.

The author would like to express his appreciation to Mitsubishi Heavy Industries, Ltd. for financial support during his year of graduate study.

ABSTRACT

The vibrations of structures in a transverse flow can be a great problem. It is well known that a strong vibration will result when the frequency of vortex shedding is close to the natural frequency of the structure. It is important to understand this "locked in" phenomenon. The Iwan-Blevins fluid-structure model has been proposed as a tool to study this phenomenon. The goal of this thesis is to extend this model by introducing a more general representation of the fluid-structure interaction force. The new model is compared with data on the lift coefficient of a circular cylinder vibrating in a steady flow and shows good agreement.

TABLE OF CONTENTS

CHAPTER I

INTRODUCTION

Vortex shedding and aerodynamic galloping are interesting features of an elastic structure exposed to a steady flow. The well known Karman vortex streets are the basis of the vortex shedding phenomenon. If the structure sheds vortices at a frequency near a harmonic of the natural frequency of the structure, vortex shedding may couple with structural vibration and generate a synchronous oscillating force on the structure. The destractive vibrations due to vortex shedding are a significant problem in many engineering systems and devices.

Flow induced oscillation is observed in tube bundles as well as for single structural elements [3]. In this case, the oscillation may be explained by the interaction of the Karman vortex street with the tube bundle. The Strouhal number in tube bundles is slightly different from 0.2 for a single cylinder and depends on the pitch-diameter ratios and the arrangements of the tubes.

This thesis is concerned with the development of a model which describes the dynamic behavior of a structural element in a flow when vortex shedding is present. It may also provide a basis for understanding the flow in tube bundles. The original model was developed by Iwan and Blevins [2]. This thesis extends this model.

In Chapter II a new model is developed based on a control volume approach to the vortex shedding process as in the original model. In Chapter III the behavior of the new model is investigated

for a stationary cylinder, a forced cylinder and an elastically mounted cylinder. In Chapter IV the model parameters are determined using experimental data for a forced cylinder. Conclusions are drawn in Chapter V.

CHAPTER II

DEVELOPMENT OF THE MODEL

2.1 The Model for the Flow

Iwan and Blevins [7] have developed a model for the vortex induced transverse vibration of an elastically mounted circular cylinder by incorporating the essential features of the gross flow behavior and relating these to the dynamic motion of an oscillating cylinder. Herein, improvements will be made on the nonlinear term of the momentum change and the force acting on the cylinder to obtain a model which more closely describes the observed behavior.

The resultant model can only approximate the complex structure-flow interaction but is nevertheless useful for identifying relevant system parameters, correlating forced vibration data, and predicting the response of untested systems.

The basic fluid mechanic assumptions of the model are

1. Inviscid flow provides a good approximation for the flow field outside the near wake.
2. Vorticity is generated only in the near wake of the cylinder. The vortices grow uniformly to a maximum strength and move down stream.
3. Two dimensional flow.
4. The force exerted on the cylinder by the flow depends only on the velocity and acceleration of the averaged flow relative to the cylinder.

The momentum equation in the y direction for the control volume shown in Figure 1 is

$$P_y = \frac{dJ_y}{dt} + S_y + F_y \qquad (2.1.1)$$

where F_y is the fluid force on the cylinder, P_y is the pressure force in the y direction on the control surface, J_y is the momentum in the control volume and S_y is the momentum change through the control volume. The pressure force P_y is given by the integration of the pressure component in the y direction along the control surface. Hence,

$$P_y = -\int_S p\,dx \cos(n,y) = -\int_{AB} p\,dx + \int_{DC} p\,dx \ . \qquad (2.1.2)$$

The momentum change through the control volume is

$$S_y = -\int_{\substack{DA \\ BC}} \rho v u\,dy + \int_{\substack{AB \\ CD}} \rho v^2\,dx \qquad (2.1.3)$$

where v and u are the vertical and horizontal components of fluid velocity respectively. ρ is the fluid density. The momentum within the control volume is

$$J_y = \iint_A \rho v\,dx\,dy \ . \qquad (2.1.4)$$

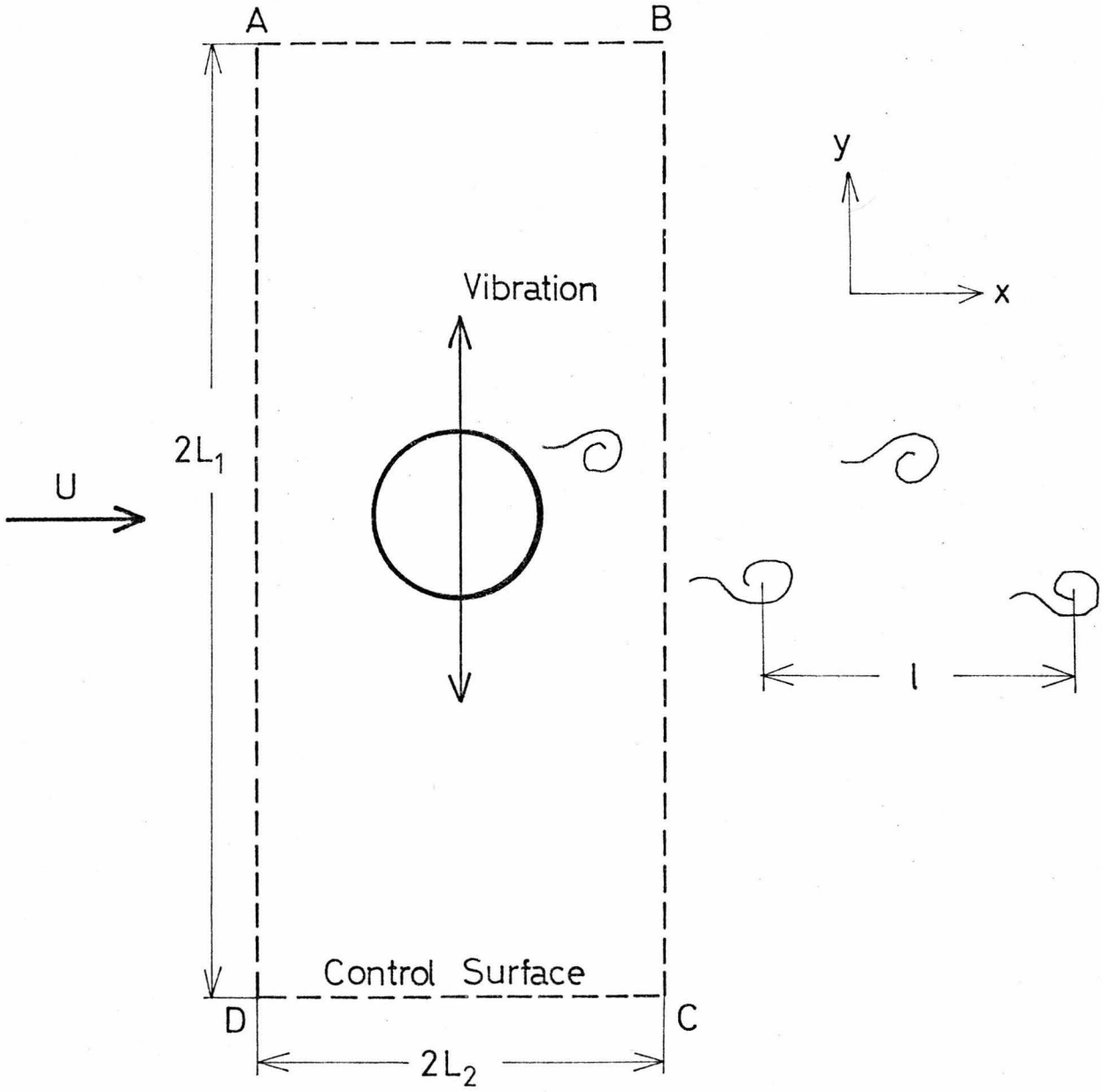

Fig. 1. Control Volume.

A weighted average of the transverse component of the flow within the control volume is defined by

$$\dot{z} \equiv \frac{J_y}{a_0 \rho D^2} , \qquad (2.1.5)$$

where D is the cylinder diameter and a_0 is a constant of proportionality.

Since the cylinder is in a uniform flow, the velocity on the boundaries AB and CD is constant, provided L_1 goes to infinity. The pressure force, therefore, is zero and

$$P_y = 0 . \qquad (2.1.6)$$

The momentum on the control surface AD is zero because $v = 0$. This also is true for the momentum components on the control surfaces AB and CD. Equation (2.1.3) therefore reduces to

$$S_y = -\int_{BC} \rho uv dy . \qquad (2.1.7)$$

Chen [1] has indicated that for a line integral bisecting an infinite vortex street $S_{y\,max} = \rho u_t \Gamma_v$ where Γ_v is the circulation of a vortex and u_t is the translational velocity of the vortex street. This result is, however, incorrect. The proper relationship is

$$S_{y\,max} = \tfrac{1}{2}\rho(U - u_t)\Gamma_v \qquad (2.1.8)$$

which is given in the Appendix. There are no vortices forward of the cylinder and S_y must have correction terms. Hence, S_y may

be taken to be of the form

$$S_y = \tfrac{1}{2}\rho(U - u_t)\Gamma + \text{correction terms} \qquad (2.1.9)$$

where Γ is the circulation of the part of a vortex which is moving out of the control volume.

The circulation of the control volume is

$$\Gamma_{cv} = \int_{\substack{DA \\ BC}} v\,dy + \int_{\substack{AB \\ CD}} u\,dx \ . \qquad (2.1.10)$$

The velocity on the boundaries AB and CD is U, so that

$$\int_{AB} u\,dx = - \int_{CD} u\,dx \ . \qquad (2.1.11)$$

The velocity component along the y axis is zero on the boundary DA. Thus, the circulation of the control volume reduces to

$$\Gamma_{cv} = \int_{BC} v\,dy \ . \qquad (2.1.12)$$

The circulation of the control volume is a function only of the induced transverse component of velocity on the surface BC. Since the circulation of a vortex going out of the control volume is the same as that of the control volume in magnitude, it is reasonable to expect the circulation of a vortex to be nearly proportional to the amplitude of the average transverse component of velocity in the control volume. That is, it is assumed that

$$\Gamma = K|\dot{z}|D \tag{2.1.13}$$

where K is the proportionality constant.

According to the Iwan-Blevins model, S_y must lag $\dot{z}$ by approximately one-quarter cycle. Since S_y is analytic and periodic at the shedding frequency, it is reasonable to assume the correction terms can be expressed in a power series of odd powers of z and $\dot{z}$ which also oscillate at the shedding frequency. For simplicity only linear and cubic terms in z and $\dot{z}$ are included in S_y. S_y is assumed to have the form

$$S_y = \tfrac{1}{2} K\rho(U - u_t)\omega_s zD - a_1\rho UD\dot{z} + a_7\rho D^2\ddot{z}$$
$$+ a_2\rho z^3U^2/D^2 + a_3\rho\dot{z}^3D/U \tag{2.1.14}$$

where a_1, a_2, a_3, a_7 and K are dimensionless constants and ω_s is the circular vortex shedding frequency.

The force exerted between the cylinder and the fluid is modeled consistent with the following assumptions:

1. The force depends only on a weighted relative velocity and acceleration of fluid and the cylinder.
2. The spectrum of frequencies known to be produced in the vortex shedding process can be approximated by a single frequency component.

The force on the cylinder which is dependent on the acceleration of the fluid and the cylinder is assumed to be linear and is represented as

$$F_{y1} = a_4 \rho D^2(\ddot{z} - \ddot{y}) + a_6 \rho D^2 \ddot{y} \qquad (2.1.15)$$

where a_4 and a_6 are dimensionless proportionality constants. It is noted that a_6 is not zero because, even if $\ddot{z}$ is equal to $\ddot{y}$, the cylinder is forced, provided $\ddot{y}$ is not zero.

The force exerted on the cylinder by the drag is a function of relative fluid velocity. The lift force is proportional to the relative angle between the free stream and the normal component of the incoming flow to the cylinder. For small displacements this angle is $(\dot{z} - \dot{y})/U$ and the lift force takes the form

$$F_{y2} = a_5 \rho DU(\dot{z} - \dot{y}) \qquad (2.1.16)$$

where a_5 is a dimensionless constant.

The net force exerted on the cylinder is the sum of F_{y1} and F_{y2} or

$$F_y = a_4 \rho D^2(\ddot{z} - \ddot{y}) + a_5 \rho DU(\dot{z} - \dot{y}) + a_6 \rho D^2 \ddot{y} \ . \qquad (2.1.17)$$

The fluid oscillator is assembled by substituting the component expressions, Eqs. (2.1.5), (2.1.6), (2.1.14) and (2.1.17), into the momentum Eq. (2.1.1). This gives

$$\begin{aligned}(a_0 + a_7)\rho D^2 \ddot{z} + \tfrac{1}{2} K \rho (U - u_t)\omega_s z/D &= a_1 \rho UD\dot{z} \\ &\quad - a_2 \rho z^3 U^2/D^2 - a_3 \rho \dot{z}^3 D/U - a_4 \rho D^2(\ddot{z} - \ddot{y}) \\ &\quad - a_5 \rho DU(\dot{z} - \dot{y}) - a_6 \rho D^2 \ddot{y} \qquad (2.1.18)\end{aligned}$$

or

$$\ddot{z} + \tfrac{1}{2} K' \left(1 - \frac{u_t}{U}\right) \frac{U}{D} \omega_s z = (a_1' - a_5') \frac{U}{D} \dot{z}$$

$$- a_2' \frac{z^3 U^2}{D^4} - a_3' \frac{\dot{z}^3}{UD} + (a_4' - a_6')\ddot{y} + a_5' \frac{U}{D} \dot{y} \qquad (2.1.19)$$

where

$$\left.\begin{aligned} K' &= \frac{K}{\hat{a}_0 + a_4} \\ a_i' &= \frac{a_i}{\hat{a}_0 + a_4} \quad , \qquad (i = 1,2,3,4,5,6) \\ \hat{a}_0 &= a_0 + a_7 \end{aligned}\right\} \qquad (2.1.20)$$

Equation (2.1.19) is of the form of a modified Van der Pol equation which additionally contains a z cube term. It describes the behavior of the fluid oscillator system around a cylinder.

2.2 The Model for the Cylinder

The vibration of an elastically mounted viscously damped cylinder is shown in Figure 2 and described by

$$m\ddot{y} + c\dot{y} + ky = F_y \qquad (2.2.1)$$

where m is the mass of the cylinder per unit length, c is the damping coefficient and k is the spring constant. The natural frequency is defined by

$$\omega_n = \sqrt{k/m} \quad . \qquad (2.2.2)$$

The structural viscous damping is defined by

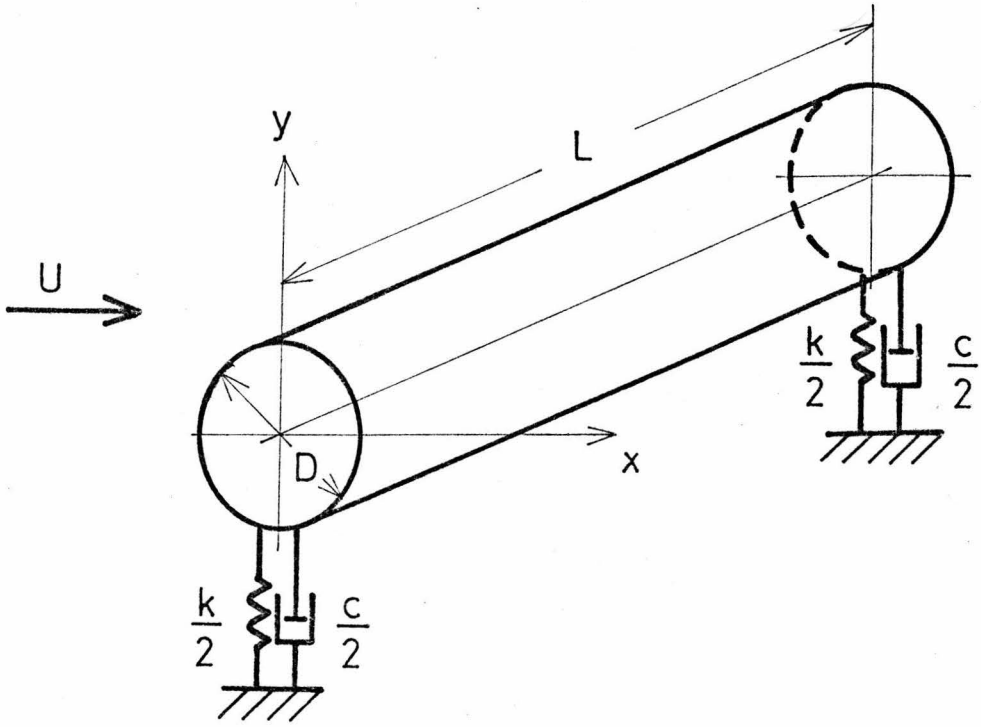

Fig. 2. Cylinder Support.

$$\xi_s = \frac{c}{2m\omega_n} \quad . \tag{2.2.3}$$

Substituting (2.1.17), (2.2.2) and (2.2.3) into Eq. (2.2.1) yields

$$m\ddot{y} + 2m\omega_n\xi_s\dot{y} + \omega_n^2 my = a_4\rho D^2(\ddot{z} - \ddot{y}) + a_5\rho DU(\dot{z} - \dot{y}) + a_6\rho D^2\ddot{y}$$

or

$$\ddot{y} + 2\xi_T\omega_y\dot{y} + \omega_y^2 y = a_4''\ddot{z} + a_5''\dot{z}\,\frac{U}{D} \tag{2.2.4}$$

where

$$\left.\begin{aligned} a_i'' &= \frac{\rho D^2 a_i}{m + (a_4 - a_6)\rho D^2} \qquad i = 4,5 \\ \omega_y &= \frac{\omega_n}{\sqrt{1 + (a_4 - a_6)\rho D^2}} \\ \xi_T &= \frac{2m\xi_s\omega_n + a_5\rho DU}{2\omega_y\{m + (a_4 - a_6)\rho D^2\}} \\ &= \frac{\xi_s\omega_n/\omega_y + \xi_f}{1 + (a_4 - a_6)\rho D^2/m} \\ \xi_f &= \frac{a_5\rho DU}{2m\omega_y} \end{aligned}\right\} \tag{2.2.5}$$

ω_y is the natural frequency of the spring-cylinder system in the fluid. ξ_T is the total damping coefficient. The latter is composed

of a component due to structural viscous damping, ξ_s, and a component due to viscous fluid damping, ξ_f, which arises from the fluid forces that dissipate the energy of the cylinder.

2.3 Characteristics of the Model

The form of the fluid oscillator Eq. (2.1.19) and the structural oscillator Eq. (2.2.4) gives the general characters of the model to be as follows:

1. The fluid/structural system has the form of two coupled autonomous oscillators.
2. The natural frequency of the fluid oscillator is given by

$$\omega_s = \tfrac{1}{2} K' \left(1 - \frac{u_t}{U}\right) \frac{U}{D} \quad . \tag{2.3.1}$$

This is also given by the consideration of shedding vortices. The frequency of shedding vortices is $\omega_s/2\pi$, thus, the velocity of vortices is $\ell\omega_s/2\pi$ in which ℓ is the pitch of the vortices. Since the translational velocity induced by a vortex street is u_t, the relative velocity of vortices with respect to the cylinder is $U - u_t$. Hence, it is true that

$$\ell \frac{\omega_s}{2\pi} = U - u_t \tag{2.3.2}$$

or

$$\omega_s = \frac{2\pi U}{\ell} \left(1 - \frac{u_t}{U}\right) \quad . \tag{2.3.3}$$

Comparison of Eq. (2.3.1) with Eq. (2.3.3) yields

$$K' = \frac{4\pi D}{\ell} \quad . \tag{2.3.4}$$

The experimental value of ℓ/D for a circular cylinder for Reynolds number of about 10^3 is, for example,

$$\frac{\ell}{D} \cong 4.26 \quad . \tag{2.3.5}$$

Substituting Eq. (2.3.5) into Eq. (2.3.4) yields

$$K' = 2.95 \quad . \tag{2.3.6}$$

The vortex shedding frequency may also be expressed in terms of the Strouhal number as

$$W_s = 2\pi S \frac{U}{D} \quad . \tag{2.3.7}$$

Equations (2.3.1) and (2.3.7) imply that K' may be expressed as

$$K' = \frac{4\pi S}{1 - u_t/U} \quad . \tag{2.3.8}$$

The Strouhal number, S, and u_t/U may be determined empirically. For a circular cylinder with Reynolds Number in the range 1×10^3 - 1×10^4 they are approximately

$$\left.\begin{aligned} S &\cong 0.189 \\ &\text{and} \\ u_t/U &\cong 0.14 \end{aligned}\right\} \qquad (2.3.9)$$

Substituting Eqs. (2.3.9) into Eq. (2.3.8) also yields $K' = 2.76$. Hence, the two expressions (2.3.1) and (2.3.7) for shedding frequency are essentially equivalent. From this point on, expression (2.3.7) will be used to express the shedding frequency.

3. The viscous damping like term in the fluid oscillator arises from vortex feedback in the near wake. In order for the fluid oscillator to have bounded amplitude, the feedback must be self limiting. That is, the feedback must be nonlinear.
4. The spring constant like term in the fluid oscillator is also nonlinear. The spring constant like term for the original model was linear.
5. Large amplitude structural oscillations are expected only if the shedding frequency is equal to or a multiple of the natural frequency of the structure so that the two oscillators are internally resonant.

To this point no restriction has been placed on the cross section which produces the vortex street. The model parameters are fixed by matching experimental data for a given cross section with the model response as predicted by analysis.

CHAPTER III

ANALYSIS OF THE MODEL

3.1 Stationary Cylinder

When the cylinder is stationary,

$$y(t) = 0 \quad . \tag{3.1.1}$$

Hence, the equation of motion, Eq. (2.1.19), reduces to

$$\ddot{z} + \omega_s^2 z = (a_1' - a_5') \frac{U}{D} \dot{z} - a_2' \frac{U^2}{D^4} z^3 - a_3' \frac{1}{UD} \dot{z}^3 \quad . \tag{3.1.2}$$

For the solution of this equation the method of slowly varying amplitude and phase will be used.

The form of the solution may be assumed to be

$$z = A_z^0(t) \cos [\omega_s t + \varphi(t)] \tag{3.1.3}$$

where the amplitude $A_z^0(t)$ and the phase angle $\varphi(t)$ are slowly varying functions of time. Substituting Eq. (3.1.3) into Eq. (3.1.2) and integrating over one period yields

$$-2\dot{A}_z^0(t) = -(a_1' - a_5') \frac{U}{D} A_z^0(t) + \tfrac{3}{4} \frac{a_3'}{UD} {A_z^0}^3(t)\omega_s^2 \tag{3.1.4}$$

and

$$2\omega_s \dot{\varphi}(t) = \tfrac{3}{4} a_2' \frac{U^2}{D^4} {A_z^0}^2(t) \quad . \tag{3.1.5}$$

The steady vibration solution is obtained by letting

$$\dot{A}_z^0(t) = 0 \quad . \tag{3.1.6}$$

This gives

$$\frac{A_z^0}{D} = \frac{[4(a_1 - a_5)/3a_3]^{\frac{1}{2}}}{2\pi S} \quad . \tag{3.1.7}$$

Substituting Eq. (3.1.7) into (3.1.5) and integrating the result yields

$$\varphi(t) = \tfrac{1}{2} \frac{a_2(a_1 - a_5)}{a_3(\hat{a}_0 + a_4)} \frac{\omega_s}{(2\pi S)^4} t + \varphi_0 \tag{3.1.8}$$

where φ_0 is a constant. The amplitude A_z^0 and the phase angle $\varphi(t)$ are respectively given by Eqs. (3.1.7) and (3.1.8). Substituting into Eq. (3.1.3) gives the hidden variable z as

$$z = \left[\frac{4(a_1 - a_5)}{3a_3}\right]^{\frac{1}{2}} \frac{D}{2\pi S} \cos(\omega_s^0 t + \varphi_0) \tag{3.1.9}$$

where the angular velocity for a stationary cylinder ω_s^0 is defined by

$$\omega_s^0 = \omega_s \left\{1 + \tfrac{1}{2} \frac{a_2(a_1 - a_5)}{a_3(a_0 + a_4)} \frac{1}{(2\pi S)^4}\right\} \quad . \tag{3.1.10}$$

Equation (3.1.9) provides a stable solution only if $(a_1 - a_3)/a_3 > 0$.

The Strouhal number for a stationary cylinder is found by using Eqs. (2.3.1), (2.3.7) and (3.1.10). This gives

$$S^0 \equiv \frac{\omega_s^0}{2\pi}\frac{D}{U} = S\left\{1 + \tfrac{1}{2}\frac{a_2(a_1 - a_5)}{a_3(\hat{a}_0 + a_4)}\frac{1}{(2\pi S)^4}\right\} . \qquad (3.1.11)$$

It will be found for realistic values of a_i that the second term on the right hand side of Eq. (3.1.11) is very small compared to 1 and is essentially negligible. This supports the assumption that $\varphi(t)$ is a slowly varying function of time. It also implies that $\omega_s^0 \cong \omega_s$ and $S^0 \cong S$.

The approximate steady-state solution for z(t) may be used to determine the circulation of the shed vortices and the lift force on a stationary cylinder. Equation (3.1.3) gives the absolute value of $\dot{z}$ as

$$|\dot{z}| = \omega_s A_z^0 . \qquad (3.1.12)$$

Substituting Eqs. (2.3.8) and (3.1.12) into Eq. (2.1.13) yields

$$\Gamma = (\hat{a}_0 + a_4)\frac{4\pi S}{1 - \frac{u_t}{U}}\omega_s A_z^0 D . \qquad (3.1.13)$$

From Eq. (2.3.7)

$$\omega_s = 2\pi S\frac{U}{D} . \qquad (3.1.14)$$

Hence,

$$\frac{\Gamma}{UD}\left(1 - \frac{u_t}{U}\right) = 2(a_0 + a_4)(2\pi S)^2\frac{A_z^0}{D} . \qquad (3.1.15)$$

Equation (3.1.15) relates the circulation of a vortex shed from a stationary cylinder and the translational velocity of that vortex street to the model parameters.

The lift force on a stationary cylinder is found by evaluating the vortex force, Eq. (2.1.17), for $y = 0$. The amplitude of the vortex force can be expressed in terms of an oscillating lift coefficient. This gives

$$C_{F_y}^0 \equiv \frac{2|F_y(y=0)|}{\rho U^2 D} = 4\pi S \left\{ a_4^2 (2\pi S)^2 + a_5^2 \right\}^{\frac{1}{2}} \frac{A_z^0}{D} \quad . \qquad (3.1.16)$$

3.2 Forced Cylinder

If the cylinder is oscillated harmonically by an external force independent of the flow surrounding it, the displacement $y(t)$ may be expressed as

$$y(t) = A_y \sin(\omega_y t - \varphi_y) \qquad (3.2.1)$$

where A_y, ω_y and φ_y are constant and will be defined by the external force acting on the cylinder. Substituting Eq. (3.2.1) into the equation of motion, Eq. (2.1.19), yields

$$\ddot{z} + \omega_s^2 z = (a_1' - a_5') \frac{U}{D} \dot{z} - a_2' \frac{U^2}{D^4} z^3 - \frac{a_3'}{UD} \dot{z}^3$$

$$- (a_4' - a_6') \omega_y^2 A_y \sin(\omega_y t - \varphi_y)$$

$$+ a_5' \frac{\omega_s}{2\pi S} \omega_y A_y \cos(\omega_y t - \varphi_y) \quad . \qquad (3.2.2)$$

In order to simplify the form of Eq. (3.2.2), let

$$\tan \varphi_y \equiv \frac{(a_4 - a_6)\omega_y D}{a_5 U} \tag{3.2.3}$$

and

$$d \equiv \left\{ (a_4' - a_6')^2 + \frac{a_5'^2 U^2}{\omega_y^2 D^2} \right\}^{\frac{1}{2}} A_y \ . \tag{3.2.4}$$

Then, Eq. (3.2.2) reduces to

$$\ddot{z} + \omega_s^2 z = (a_1' - a_5') \frac{U}{D} \dot{z} - a_2' \frac{U^2}{D^4} z^3 - \frac{a_3'}{UD} \dot{z}^3$$

$$+ d\omega_y^2 \cos \omega_y t \ . \tag{3.2.5}$$

A solution of Eq. (3.2.5) may be assumed of the form

$$z = b_1(t) \cos \omega_y t + b_2(t) \sin \omega_y t \tag{3.2.6}$$

where $b_1(t)$ and $b_2(t)$ are slowly varying functions of time. Substituting Eq. (3.2.6) into Eq. (3.2.5) and performing a harmonic balance produces the following variational equations:

$$\frac{2}{\beta} \frac{dx}{dt} = x(1 - r^2) + y(\sigma + \rho r^2) \ , \tag{3.2.7}$$

and

$$\frac{2}{\beta} \frac{dy}{dt} = y(1 - r^2) - x(\sigma + \rho r^2) + F \tag{3.2.8}$$

where

$$x \equiv \left\{\frac{3a_3}{4(a_1 - a_5)}\right\}^{\frac{1}{2}} \frac{\omega_y}{U} b_1(t) \quad , \tag{3.2.9}$$

$$y \equiv \left\{\frac{3a_3}{4(a_1 - a_5)}\right\}^{\frac{1}{2}} \frac{\omega_y}{U} b_2(t) \quad , \tag{3.2.10}$$

$$\beta \equiv (a_1' - a_5') \frac{U}{D} \quad , \tag{3.2.11}$$

$$\sigma \equiv \frac{(\omega_s^2 - \omega_y^2)D}{(a_1' - a_5')\omega_y U} \quad , \tag{3.2.12}$$

$$\rho \equiv \frac{a_2 U^3}{a_3 (D\omega_y)^3} \quad , \tag{3.2.13}$$

$$F \equiv \left\{\frac{3a_3'}{4(a_1' - a_5')}\right\}^{\frac{1}{2}} \frac{d}{D}\left(\frac{\omega_y D}{U}\right)^2 \quad , \tag{3.2.14}$$

and

$$r^2 = x^2 + y^2 \quad . \tag{3.2.15}$$

The steady state solutions to Eqs. (3.2.7) and (3.2.8) are given by setting $\dot{b}_1(t) = \dot{b}_2(t) = 0$ or

$$\frac{dx}{dt} = \frac{dy}{dt} = 0 \quad . \tag{3.2.16}$$

Substituting Eqs. (3.2.16) into Eqs. (3.2.7) and (3.2.8) gives

$$x(1 - r^2) + y(\sigma + \rho r^2) = 0 \quad , \tag{3.2.17}$$

and

$$x(\sigma+\rho r^2) - y(1-r^2) = F \quad . \tag{3.2.18}$$

Equations (3.2.17) and (3.2.18) are easily solved for x and y to give

$$x = \frac{r^2(\sigma+\rho r^2)}{F} \quad , \tag{3.2.19}$$

and

$$y = -\frac{r^2(1-r^2)}{F} \quad . \tag{3.2.20}$$

These equations can be combined as

$$r^2\{(\sigma+\rho r^2)^2 + (1-r^2)^2\} = F^2 \quad . \tag{3.2.21}$$

The amplitude of the solution is found by solving the cubic equation (3.2.21) numerically and substituting the result into Eqs. (3.2.19) and (3.2.20) which determine b_1 and b_2.

In order to investigate the stability of the steady-state solution, consider a small perturbation of the form

$$x = x_0 + \xi \quad ,$$

and

$$y = y_0 + \eta \quad , \tag{3.2.22}$$

where x_0 and y_0 are the steady-state solutions and ξ and η are the small perturbations. Let

$$r_0^2 = x_0^2 + y_0^2 \quad , \tag{3.2.23}$$

then

$$r^2 = r_0^2 + (\xi x_0 + \eta y_0) + (\xi^2 + \eta^2)$$

$$\doteq r_0^2 + 2(\xi x_0 + \eta y_0) \quad . \tag{3.2.24}$$

Substituting Eqs. (3.2.22) and (3.2.24) into Eqs. (3.2.7) and (3.2.8) gives

$$\frac{d\underline{\xi}}{dt} = A\underline{\xi} \tag{3.2.25}$$

where

$$\underline{\xi} = \begin{pmatrix} \xi \\ \eta \end{pmatrix} \tag{3.2.26}$$

and

$$A = \frac{(a_1' - a_5')\omega_s}{4\pi S} \begin{bmatrix} 1 - r_0^2 - 2x_0^2 + 2\rho x_0 y_0 & \sigma - 2x_0 y_0 + \rho r_0^2 + 2\rho y_0^2 \\ -\sigma - 2x_0 y_0 - \rho r_0^2 - 2\rho x_0^2 & 1 - r_0^2 - 2y_0^2 - 2\rho x_0 y_0 \end{bmatrix}$$

(3.2.27)

Hence, the condition for stability is

$$T_r(A) = \frac{(a_1' - a_5')U}{D}(1 - 2r_0^2) < 0 \tag{3.2.28}$$

or

$$r_0^2 < \tfrac{1}{2} \quad . \tag{3.2.29}$$

The character of the singular points is shown in Table 1. Figures 3 show the square of the amplitude r^2 as a function of ρ, σ and F. If a_2 is zero, ρ is also zero. In this case, the simple harmonic solution becomes unstable if $r^2 < \frac{1}{2}$ for $F^2 > 8/27$.

However, if a_2 is not zero, it is more complicated as shown in Figs. 3(b)-(e). a_2, that is ρ, deforms the shape of the curves. The bigger $|\rho|$, the greater the deformation of the curves.

It may be shown that there are two criteria which determine the stability boundaries. These are

(1) $r^2 = \frac{1}{2}$, and

(2) $|A| = \frac{\beta^2}{4}\{\sigma^2 + 6\rho\sigma r^2 + 3\rho^2 r^4 + (1-r^2)(1-3r^2)\} = 0$ and

$$\{T_r(A)\}^2 - 4|A| = \beta^2\{(1-3\rho^2)r^4 - 6\rho\sigma r^2 - \sigma^2\} > 0 \ .$$

Using Eq. (3.2.21), condition (1) gives

$$(\sigma + \tfrac{1}{2}\rho)^2 + \tfrac{1}{4} = 2F^2 \ . \tag{3.2.30}$$

The other condition (2) gives

$$45\rho^4\sigma^2 - 18\rho^4\sigma + 9\rho^4 + 9\rho^3\sigma - 57\rho^2\sigma^2 - 51\rho\sigma$$

$$-12\rho^2 - 12\sigma^2 + 3 \pm (2 - 6\rho^2 - 18\rho^3\sigma - 18\rho\sigma)\sqrt{D} > 0 \tag{3.2.31}$$

provided

$$\rho\sigma < \tfrac{2}{3} \ , \tag{3.3.32}$$

and

$$D \equiv 6\rho^2\sigma^2 - 12\rho\sigma - 3\rho^2 - 3\sigma^2 + 1 > 0 \ . \tag{3.2.33}$$

In the case that Eq. (3.2.32) or (3.2.33) is not satisfied, the condition (2) can be neglected.

$\{T_r(A)\}^2 - 4\|A\|$	$\|A\|$	r_0^2	Characters	Stability
> 0	> 0	$> \frac{1}{2}$	Node	Stable
		$< \frac{1}{2}$	Node	Unstable
	< 0		Saddle	Unstable
< 0		$> \frac{1}{2}$	Spiral	Stable
		$< \frac{1}{2}$	Spiral	Unstable
		$= \frac{1}{2}$	Center	
$= 0$		$> \frac{1}{2}$	Node	Stable
		$< \frac{1}{2}$	Node	Unstable

$$\{T_r(A)\}^2 - 4|A| = \beta^2\{(1-3\rho^2)r_0^4 - 6\rho\sigma r_0^2 - \sigma^2\}$$

$$|A| = \frac{\beta^2}{4}\{\sigma^2 + 6\rho\sigma r_0^2 + 3\rho^2 r_0^4 + (1-r_0^2)(1-3r_0^2)\}$$

Table 1. The Characters of the Singular Points

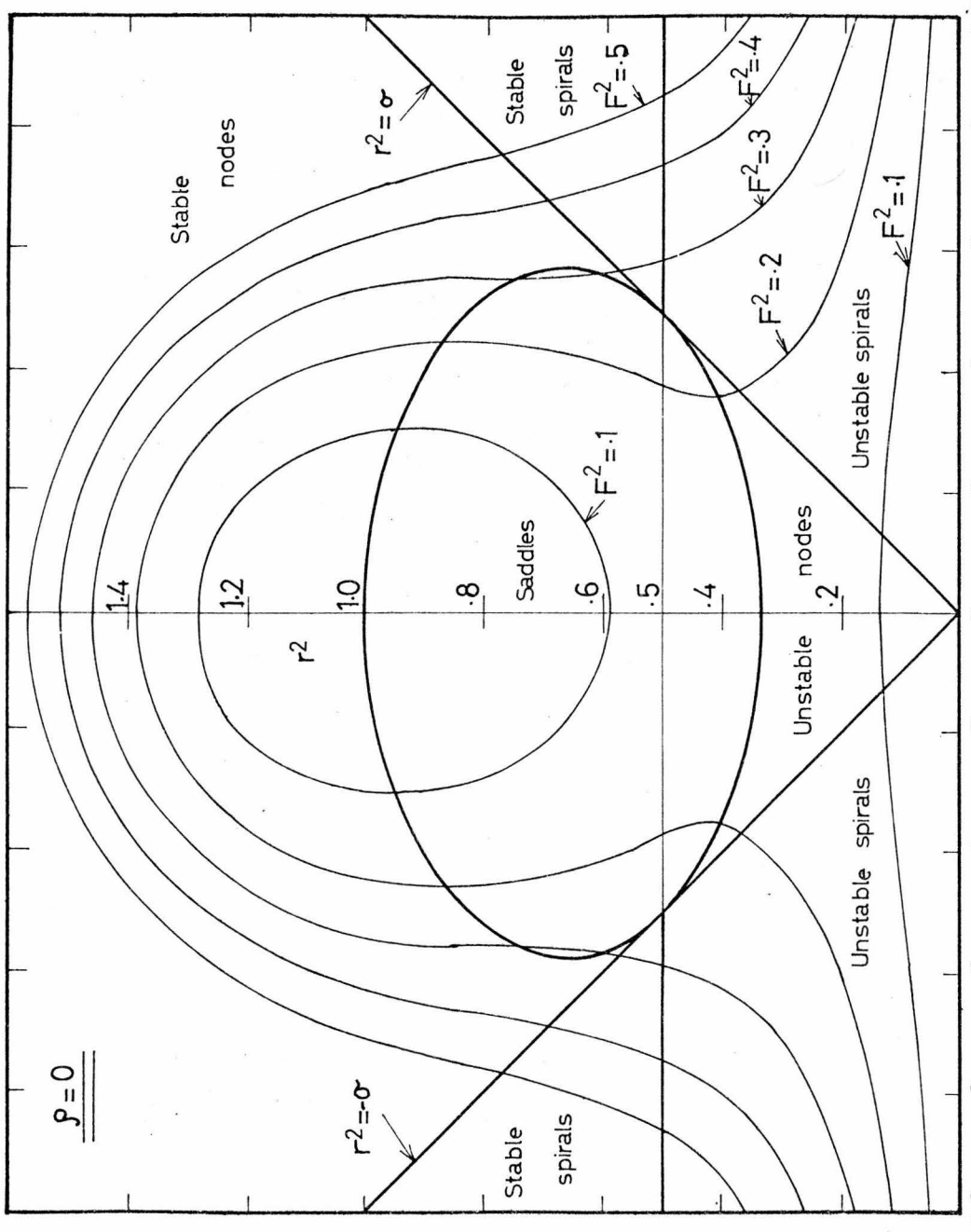

Fig. 3(a). Response of Forced Oscillator with $\rho=0$.
(Van der Pol Oscillator)

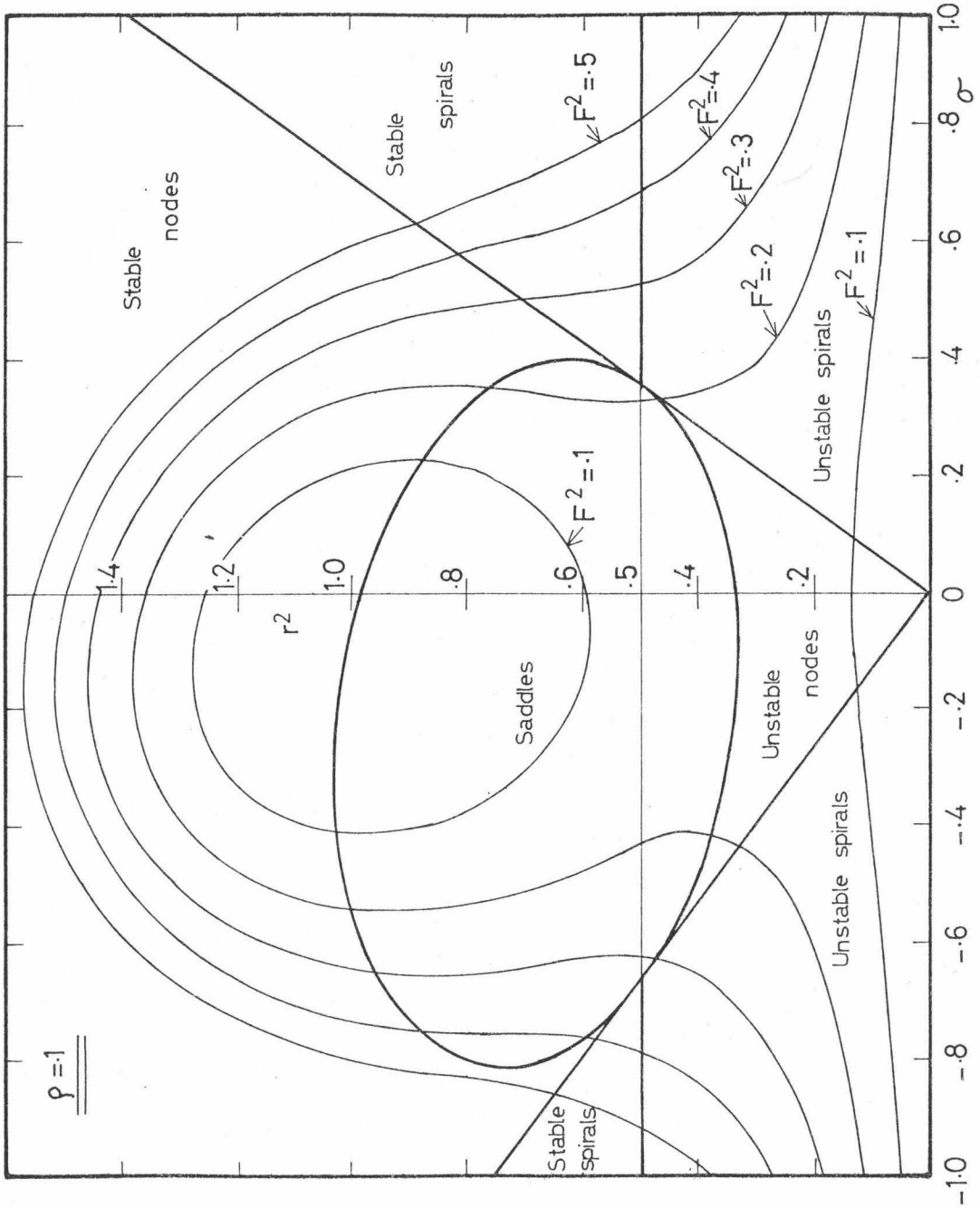

Fig. 3(b). Response of Forced Oscillator with ρ=.1.

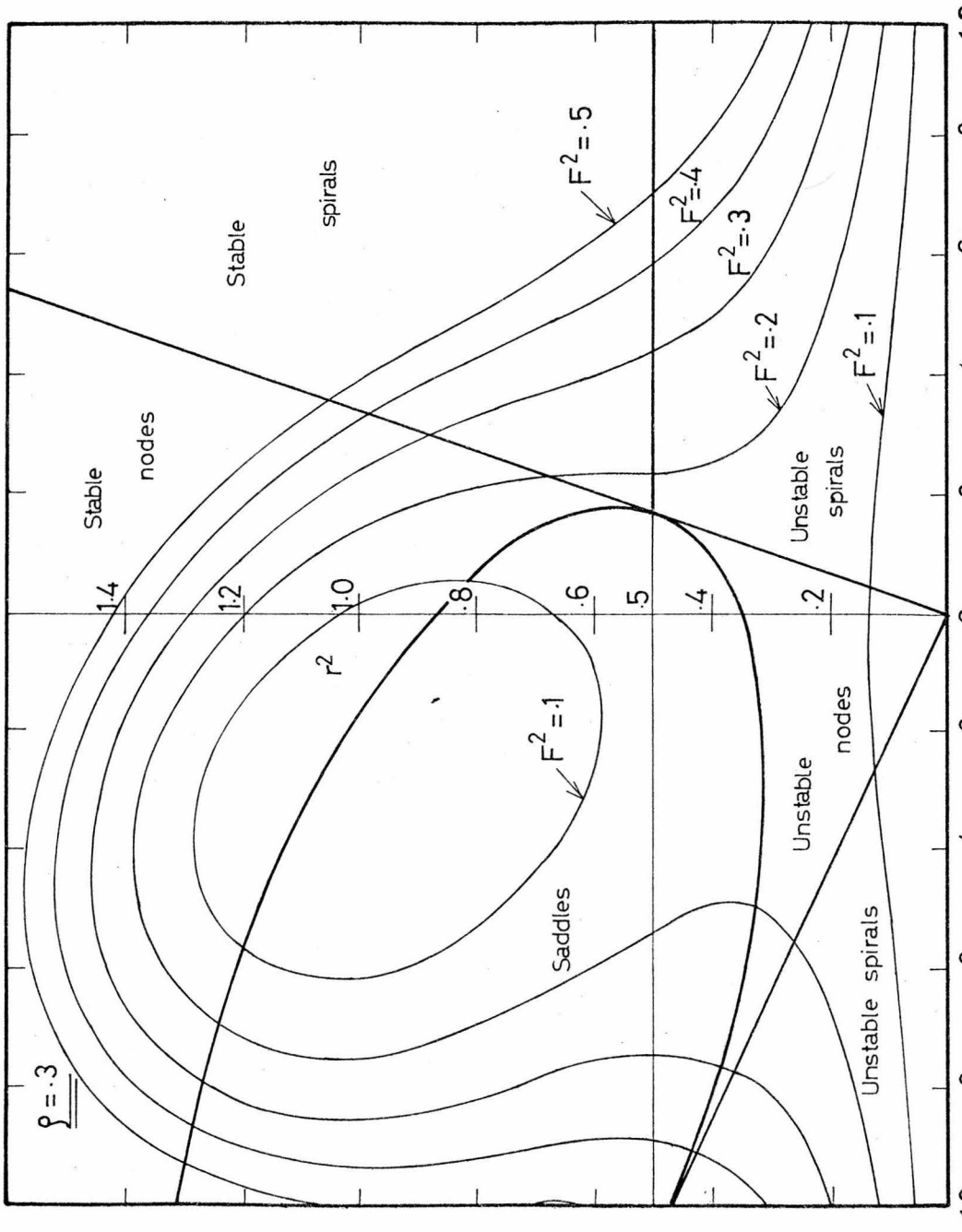

Fig. 3(d) Response of Forced Oscillator with ρ=.3.

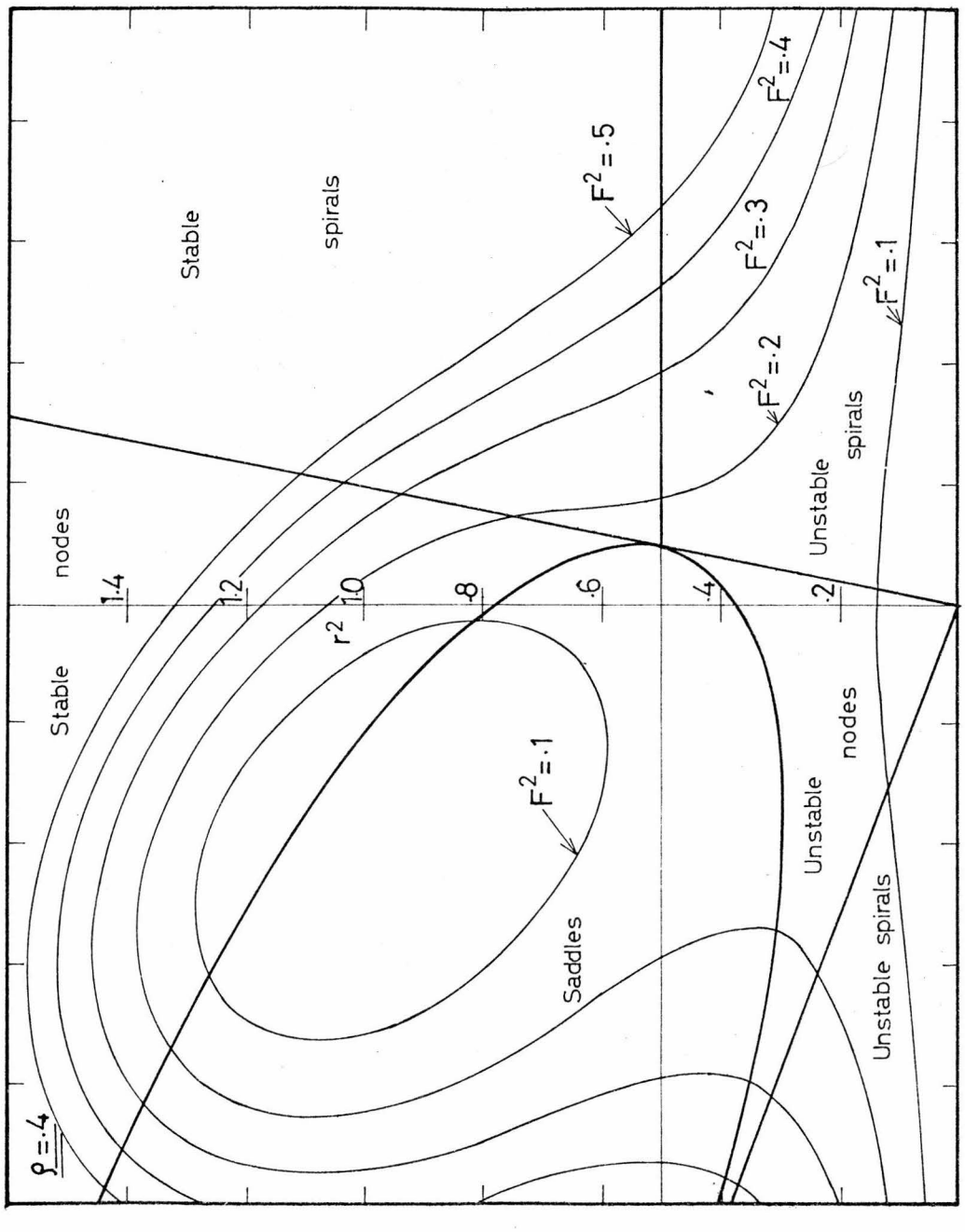

Fig. 3(e). Response of Forced Oscillator with ρ=.4.

The lift coefficient of the cylinder will be examined next. Let the relative velocity z - y be of the form

$$z - y = \bar{A} \sin (\omega_y t + \bar{\varphi}) \tag{3.2.34}$$

where $\bar{A}$ and $\bar{\varphi}$ are constants. Substituting Eqs. (3.2.1) and (3.2.34) into Eq. (2.1.17) gives the lift force as

$$\begin{aligned} F_y = & - a_4 \rho D^2 \bar{A} \omega_y^2 \sin (\omega_y t + \bar{\varphi}) \\ & + a_5 \rho D U \bar{A} \omega_y \cos (\omega_y t + \bar{\varphi}) \\ & - a_6 \rho D^2 A_y \omega_y^2 \sin (\omega_y t - \varphi_y) \ . \end{aligned} \tag{3.2.35}$$

Hence, the maximum amplitude of F_y is

$$|F_y|_{max} = \rho U D \bar{A} \omega_y \left[\left\{ \frac{a_4^2 (D\omega_y)^2}{U^2} + a_5^2 \right\}^{\frac{1}{2}} + |a_6| \frac{D\omega_y}{U} \right] \ . \tag{3.2.36}$$

The lift coefficient is therefore

$$C_{F_y} \equiv \frac{2|F_y|_{max}}{\rho U^2 D} = \frac{2\bar{A}\omega_y}{U} \left[\left\{ \frac{a_4^2 (D\omega_y)^2}{U^2} + a_5^2 \right\}^{\frac{1}{2}} + |a_6| \frac{D\omega_y}{U} \right] \ . \tag{3.2.37}$$

$\bar{A}$ and $\bar{\varphi}$ will next be given. Substituting Eqs. (3.2.1) and (3.2.6) into Eq. (3.2.34) yields

$$\begin{aligned} \bar{A} \sin (\omega_y t + \bar{\varphi}) = & (b_1 + A_y \sin \varphi_y) \cos \omega_y t \\ & + (b_2 - A_y \cos \varphi_y) \sin \omega_y t \ . \end{aligned} \tag{3.2.38}$$

Thus, $\overline{A}$ and $\overline{\varphi}$ are respectively expressed by

$$\overline{A} = [(b_1 + A_y \sin\varphi_y)^2 + (b_2 - A_y \cos\varphi_y)^2]^{\frac{1}{2}} \qquad (3.2.39)$$

and

$$\tan\overline{\varphi} = \frac{b_1 + A_y \sin\varphi_y}{b_2 - A_y \cos\varphi_y} \ . \qquad (3.2.40)$$

Equation (3.2.3) gives φ_y and Eqs. (3.2.9) and (3.2.10) give b_1 and b_2. Using these equations and Eqs. (3.2.19) and (3.2.20), the amplitude $\overline{A}$ is at last expressed by

$$\frac{\overline{A}}{D} = \left[\left\{\gamma_1 \frac{r^2(\sigma+\rho r^2)}{F} + \gamma_2 \frac{A_y}{D}\right\}^2 + \left\{\gamma_1 \frac{r^2(1-r^2)}{F} + \gamma_3 \frac{A_y}{D}\right\}^2\right]^{\frac{1}{2}} \qquad (3.2.41)$$

where

$$\gamma_1 \equiv \left[\frac{a_1 - a_5}{3a_3}\right]^{\frac{1}{2}} \frac{2U}{D\omega_y} \qquad (3.2.42)$$

$$\gamma_2 \equiv \frac{(a_0 + a_4)(a_4 - a_6)\omega_y}{|a_0 + a_4|\sqrt{(a_4 - a_6)^2\omega_y^2 + (a_5\ U/D)^2}} \qquad (3.2.43)$$

$$\gamma_3 \equiv \frac{(a_0 + a_4)(a_5\ U/D)}{|a_0 + a_4|\sqrt{(a_4 - a_6)^2\omega_y^2 + (a_5\ U/D)^2}} \qquad (3.2.44)$$

σ, ρ, F and r are given by Eqs. (3.2.12) - (3.2.15). Thus, $\overline{A}$ is given by Eq. (3.2.41) for the diameter of the cylinder, D, the

velocity, U, the amplitude and the angular velocity of the cylinder vibration, A_y and ω_y, provided the parameters, a_0, a_1, a_2, a_3, a_4, a_5 and a_6, are known.

3.3 Elastically Mounted Cylinder

The coupled oscillator equations for an elastically mounted cylinder are given by Eqs. (2.1.19) and (2.2.5) which are

$$\ddot{z} + \tfrac{1}{2}K'\left(1 - \frac{u_t}{U}\right)\frac{U}{D}\,\omega_s z =$$

$$(a_1' - a_5')\frac{U}{D}\dot{z} - a_2'\frac{z^3U^2}{D^4} - a_3'\frac{\dot{z}^3}{UD} + (a_4' - a_6')\ddot{y} + a_5'\frac{U}{D}\dot{y} \qquad (3.3.1)$$

and

$$\ddot{y} + 2\xi_T\omega_y\dot{y} + \omega_y^2 y = a_4''\ddot{z} + a_5''\dot{z}\,\frac{U}{D}\,. \qquad (3.3.2)$$

These equations are solved for steady state by assuming a harmonic solution form:

$$z = A_z \cos(\omega t + \varphi_z) \qquad (3.3.3)$$

where A_z, ω and φ_z are constants. The nonlinear differential equation describing the cylinder motion (3.3.1) is then solved for the cylinder displacement in terms of the harmonic fluid oscillations. The cylinder displacement as a function of the fluid oscillations can then be substituted back into the fluid oscillator equation to produce a single nonlinear autonomous differential equation which may be solved by asymptotic methods.

Equation (3.3.3) is substituted into Eq. (3.3.2) to give

$$\ddot{y} + 2\xi_T\omega\dot{y} + \omega_y^2 y = -a_4''A_z\omega^2\cos(\omega t+\varphi_z) - a_5''\frac{U}{D}A_z\omega\sin(\omega t+\varphi_z) \quad . \tag{3.3.4}$$

Let

$$y = b_1\cos(\omega t + \varphi_z) + b_2\sin(\omega t + \varphi_z) \quad , \tag{3.3.5}$$

then, Eq. (3.3.4) is solved to give:

$$y = \{-a_4''(\omega_y^2 - \omega^2) + \xi_T\omega_y\omega_s a_5''/\pi S\}\omega^2 AFz + \{2a_4''\xi_T\omega_n\omega^2 + a_5''\omega_s(\omega_n^2 - \omega^2)/2\pi S\}AF\dot{z} \tag{3.3.6}$$

where the amplification factor is denoted by AF.

$$AF \equiv 1/\{(\omega_y^2 - \omega^2)^2 + 4\xi_T^2\omega_y^2\omega^2\} \quad . \tag{3.3.7}$$

The amplitude of the cylinder displacement is given by Eq. (3.3.6) as

$$A_y = A_z AF^{\frac{1}{2}}[a_4''^2(\omega/\omega_y)^4 + a_5''^2(\omega_s/\omega_y)^2(\omega/\omega_y)^2/(2\pi S)^2]^{\frac{1}{2}}\omega_y^2 \quad . \tag{3.3.8}$$

Equation (3.3.6) is substituted into the fluid oscillator equation (3.3.1) to produce the single nonlinear equation.

$$\ddot{z} + \omega_s^2 z = \alpha_1\dot{z} + \alpha_2\ddot{z} + \alpha_3\dddot{z} - \alpha_4 z^3 - \alpha_5\dot{z}^3 \tag{3.3.9}$$

where

$$
\left.
\begin{aligned}
\alpha_1 &\equiv (a_1' - a_5')\frac{U}{D} + a_5'\frac{U}{D}\{-a_4''(\omega_y^2 - \omega^2) + a_5''\xi_T\omega_y\omega_s/\pi S\}\omega^2 AF \,, \\
\alpha_2 &\equiv a_5'\frac{U}{D}\{2a_4''\xi_T\omega_y\omega^2 + a_5''\omega_s(\omega_y^2 - \omega^2)/2\pi S\}AF \\
&\quad + (a_4' - a_6')\left\{-a_4''(\omega_y^2 - \omega^2) + \frac{a_5''\xi_T\omega_y\omega_s}{\pi S}\right\}\omega^2 AF \,, \\
\alpha_3 &\equiv (a_4' - a_6')\left\{2a_4''\xi_T\omega_y\omega^2 + \frac{a_5''\omega_s(\omega_y^2 - \omega^2)}{2\pi S}\right\}AF \,, \\
\alpha_4 &\equiv a_2'\frac{U^2}{D^3} \,, \\
\alpha_5 &\equiv a_3'\frac{\dot{z}^3}{UD} \,.
\end{aligned}
\right\} \quad (3.3.10)
$$

Equation (3.3.9) is the approximate equation which expresses the steady-state oscillation. Next, the stability conditions of this system will be examined.

The solution of Eq. (3.3.9) is assumed to be oscillatory of the form

$$z = A_z(t)\cos[\omega t + \varphi_z(t)] \qquad (3.3.11)$$

where $A_z(t)$ and $\varphi(t)$ are slowly varying functions in time and the α_i are assumed to be small parameters. The method of slowly varying parameters and the harmonic balance technique give:

$$\dot{A}_z(t) = [\alpha_1^* + \alpha_3^* A_z^2(t)]A_z(t) \,, \qquad (3.3.12)$$

$$\dot{\varphi}_z(t) = [\alpha_2^* - \alpha_4^* A_z^2(t)] \qquad (3.3.13)$$

where

$$\left.\begin{aligned}
\alpha_1^* &\equiv \frac{\alpha_1(1-\alpha_2) + \alpha_3(1-\alpha_2)\omega^2 - 2\alpha_3\omega_s^2}{(\alpha_2-1)^2 + (2\alpha_3\omega)^2} \quad , \\
\alpha_2^* &\equiv \frac{-2\alpha_3^2\omega^4 + \{2\alpha_1\alpha_3 - (\alpha_2-1)^2\}\omega^2 - (\alpha_2-1)\omega_s^2}{\omega\{(\alpha_2-1)^2 + (2\alpha_3\omega)^2\}} \quad , \\
\alpha_3^* &\equiv \frac{3\{\alpha_5\omega^2(\alpha_2-1) + 2\alpha_3\alpha_4\}}{4\{(\alpha_2-1)^2 + (2\alpha_3\omega)^2\}} \quad , \\
\alpha_4^* &\equiv \frac{3\{2\alpha_3\alpha_5\omega^4 + \alpha_4(\alpha_2-1)\}}{4\omega\{(\alpha_2-1)^2 + (2\alpha_2\omega)^2\}} \quad .
\end{aligned}\right\} \qquad (3.3.14)$$

The steady-state solution is obtained by setting $\dot{A}_z(t) = 0$. Then, for nontrivial solutions, Eq. (3.3.12) yields

$$A_z = \left(-\frac{\alpha_1^*}{\alpha_3^*}\right)^{\frac{1}{2}} \quad . \qquad (3.3.15)$$

The phase angle in this case is

$$\varphi_z(t) = (\alpha_2^* - \alpha_4^* A_z^2)t + \varphi_z^0 \qquad (3.3.16)$$

where φ_z^0 is a constant. The amplitude A_z^0 and the phase angle are given by Eq. (3.3.15) and (3.3.16). These are substituted into Eq. (3.3.11) to yield

$$z = \left(- \frac{\alpha_1^*}{\alpha_3^*} \right)^{\frac{1}{2}} \cos (\omega t + \varphi_z^0) \tag{3.3.17}$$

where

$$\omega = \omega^0 + \alpha_2^* + \frac{\alpha_1^* \alpha_4^*}{\alpha_3^*} \quad . \tag{3.3.18}$$

ω^0 is the order one estimate of the frequency of oscillation.

Since the α_i have been assumed to be small, the α_i^* are also small parameters by Eq. (3.3.14). The second and the third terms on the right hand side of Eq. (3.3.18) are, therefore, also small. This supports the assumption that $\varphi_z(t)$ is a slowly varying function. Equation (3.3.18) determines the frequency of the cylinder and fluid oscillation. This transcendental frequency equation is decoupled from Eq. (3.3.15) which determines the amplitude of the fluid oscillator. The frequency equation can be solved numerically. The resultant frequency, ω, is substituted into Eq. (3.3.15) to determine the amplitude of the elastically mounted cylinder displacement due to vortex shedding.

For stable oscillation Eq. (3.3.15) also requires the condition

$$- \frac{\alpha_1^*}{\alpha_3^*} > 0 \tag{3.3.19}$$

or

$$\left.\begin{array}{l} \alpha_1^* > 0 \\ \alpha_3^* < 0 \end{array} \right\} \quad \text{and} \tag{3.3.20}$$

by Eqs. (3.3.10) and (3.3.14). This condition is satisfied by the assumption that α_i are small values.

CHAPTER IV

DETERMINATION OF THE MODEL PARAMETERS - CIRCULAR CYLINDER

Once the fluid-structure model for cylinder vibration has been developed, the seven constants a_i ($i = 0, 1, 2, 3, \ldots, 6$) can be determined by experimental data. Recently, Sarpkaya [4] has made measurements of the vortex induced forces on a forced circular cylinder in a transverse flow. The results of this experimental investigation have been presented in the form of effective transverse inertia and drag coefficients. These results will be used to determine the parameters of the proposed model.

4.1 Effective Inertia and Drag Coefficients

The force acting on the cylinder in the y-direction, F_y, may be expressed in terms of a dimensionless inertia coefficient, C_{mL} and drag coefficient C_{dL} as

$$\frac{F_y}{0.5\rho DU^2} = C_{mL}\pi^2\left(\frac{U_m T}{D}\right)\left(\frac{D}{UT}\right)^2 \sin\frac{2\pi}{T}t' - C_{dL}\left(\frac{U_m T}{D}\right)^2\left(\frac{D}{UT}\right)^2 \left|\cos\frac{2\pi}{T}t'\right| \cos\frac{2\pi}{T}t' \qquad (4.1.1)$$

where C_{mL} and C_{dL} are given by their Fourier averages as

$$C_{mL} = \frac{2U_m T}{\pi^3 D}\int_0^{2\pi} (F_y \sin\theta)d\theta/(\rho U_m^2 D) \qquad (4.1.2)$$

$$C_{dL} = -\frac{3}{4}\int_0^{2\pi} (F_y \cos\theta)d\theta/(\rho U_m^2 D) \qquad (4.1.3)$$

and

$$\theta = \frac{2\pi}{T} t' \ .$$

U_m is the amplitude of the cylinder velocity and T is the period of the cylinder vibration so that the instantaneous velocity of the cylinder is

$$v = -U_m \cos\theta \ . \qquad (4.1.4)$$

The relationship between the seven constants, a_i, and the Fourier coefficients C_{mL} and C_{dL} may be obtained as follows.

The displacement y has been defined as

$$y = A_y \sin(\omega_y t - \varphi_y) \ . \qquad (4.1.5)$$

Hence, the velocity of the cylinder caused by the vibration is

$$v = \frac{dy}{dt} = A_y\omega_y \cos(\omega_y t - \varphi_y) \ . \qquad (4.1.6)$$

Comparison of Eq. (4.1.6) with Eq. (4.1.4) yields

$$U_m = -A_y\omega_y \ , \qquad (4.1.7)$$

$$\theta = \omega_y t - \varphi_y \ . \qquad (4.1.8)$$

The period of the cylinder vibration is obviously given by

$$T = \frac{2\pi}{\omega_y} \ . \qquad (4.1.9)$$

The force acting on the cylinder F_y has been expressed by Eq. (3.2.35) as

$$F_y = - a_4 \rho D^2 \bar{A} \omega_y^2 \sin(\omega_y t + \bar{\varphi}) + a_5 \rho D U \bar{A} \omega_y \cos(\omega_y t + \bar{\varphi}) - a_6 \rho D^2 A_y \omega_y^2 \sin(\omega_y t - \varphi_y) \quad . \tag{4.1.10}$$

Substituting Eqs. (4.1.7), (4.1.8), (4.1.9) and (4.1.10) into Eqs. (4.1.2) and (4.1.3) determines the expressions of the Fourier coefficients C_{mL} and C_{dL} as follows:

$$C_{mL} = \frac{4\bar{A}}{\pi A_y} \left\{ a_4 \cos(\bar{\varphi} + \varphi_y) + a_5 \frac{U}{D\omega_y} \sin(\bar{\varphi} + \varphi_y) \right\} + \frac{4}{\pi} a_6 \quad , \tag{4.1.11}$$

and

$$C_{dL} = \frac{3\pi \bar{A} D}{4 A_y^2} \left\{ a_4 \sin(\bar{\varphi} + \varphi_y) - a_5 \frac{U}{D\omega_y} \cos(\bar{\varphi} + \varphi_y) \right\} \quad . \tag{4.1.12}$$

The relative amplitude $\bar{A}$ of $z - y$ has been given by Eq. (3.2.34). The ratio of the relative amplitude $\bar{A}$ to the amplitude of the cylinder vibration A_y is given by Eq. (3.2.41) and

$$\frac{\bar{A}}{A_y} = \left[\left\{ \gamma_1 r^2 (\sigma + \rho r^2) + \gamma_2 \frac{F A_y}{D} \right\}^2 + \left\{ \gamma_1 r^2 (1 - r^2) + \gamma_3 \frac{F A_y}{D} \right\}^2 \right]^{\frac{1}{2}} \left(|F| \frac{A_y}{D} \right) . \tag{4.1.13}$$

The terms $\sin(\bar{\varphi} + \varphi_y)$ and $\cos(\bar{\varphi} + \varphi_y)$ may be determined from Eqs. (3.2.9), (3.2.6), (3.2.10) and (3.2.40) as follows:

$$\sin(\bar{\varphi} + \varphi_y) = -\frac{A_y}{\bar{A}}\left[\gamma_3\left\{\frac{\gamma_1 r^2(\sigma+\rho r^2)D}{FA_y} + \gamma_2\right\} - \gamma_2\left\{\frac{\gamma_1 r^2(1-r^2)D}{FA_y} + \gamma_3\right\}\right] \tag{4.1.14}$$

and

$$\cos(\bar{\varphi}+\varphi_y) = \frac{A_y}{\bar{A}}\left[\gamma_3\left\{\frac{\gamma_1 r^2(1-r^2)D}{FA_y} + \gamma_3\right\} + \gamma_2\left\{\frac{\gamma_1 r^2(\sigma+\rho r^2)D}{FA_y} + \gamma_2\right\}\right] . \tag{4.1.15}$$

The third term on the right hand side of Eq. (4.1.11) is a constant which shifts the value of C_{mL} upward or downward.

Providing the coefficients a_0, a_1, a_2, a_3, a_4, a_5 and a_6, γ_1, γ_2 and γ_3 are given by Eqs. (3.2.42), (3.2.43) and (3.2.44) for $U/D\omega_y$. σ and ρ are given by Eqs. (3.2.12) and (3.2.13). F is given by Eq. (3.2.14) for d/D which is defined by Eq. (3.2.4). Consequently, C_{dL} and C_{mL} may be calculated through Eqs. (4.1.13), (4.1.14), (4.1.15), (4.1.11)aand (4.1.12) for the amplitude A_y/D and the reduced velocity $U/D\omega_y$.

4.2 Determination of Model Parameters

Figure 4(a) through 4(c) shows Sarpkaya's experimental results [4] for the inertia and drag coefficients as a function of dimensionless flow velocity $2\pi U/\omega_y D$ for three different values of A_y/D. The model parameters $a_0, \ldots, a_6$ were selected so as to

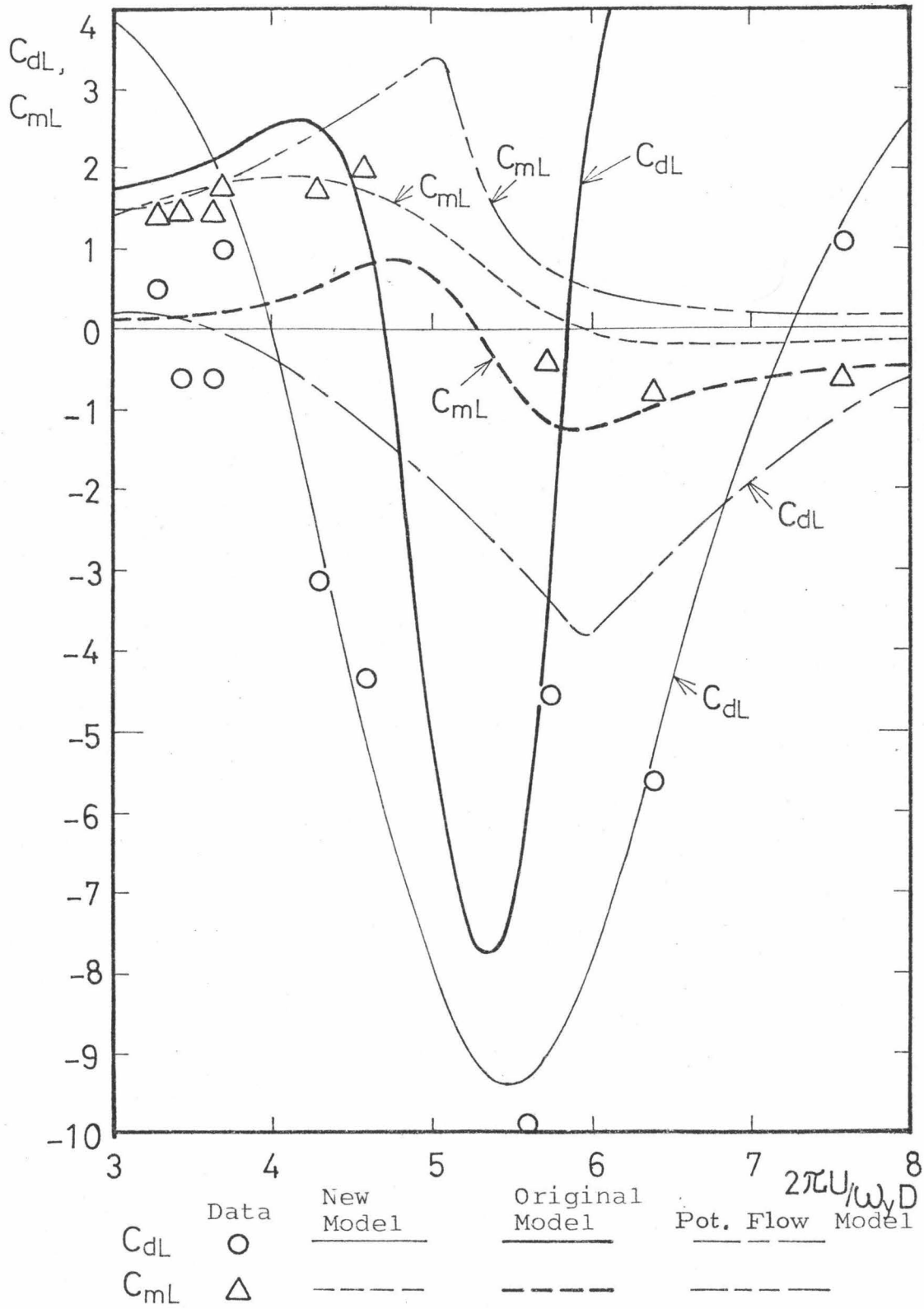

Fig. 4(a). The Lift Coefficients, C_{dL} & C_{mL}, in the Resonance Range with A_y/D = .25.

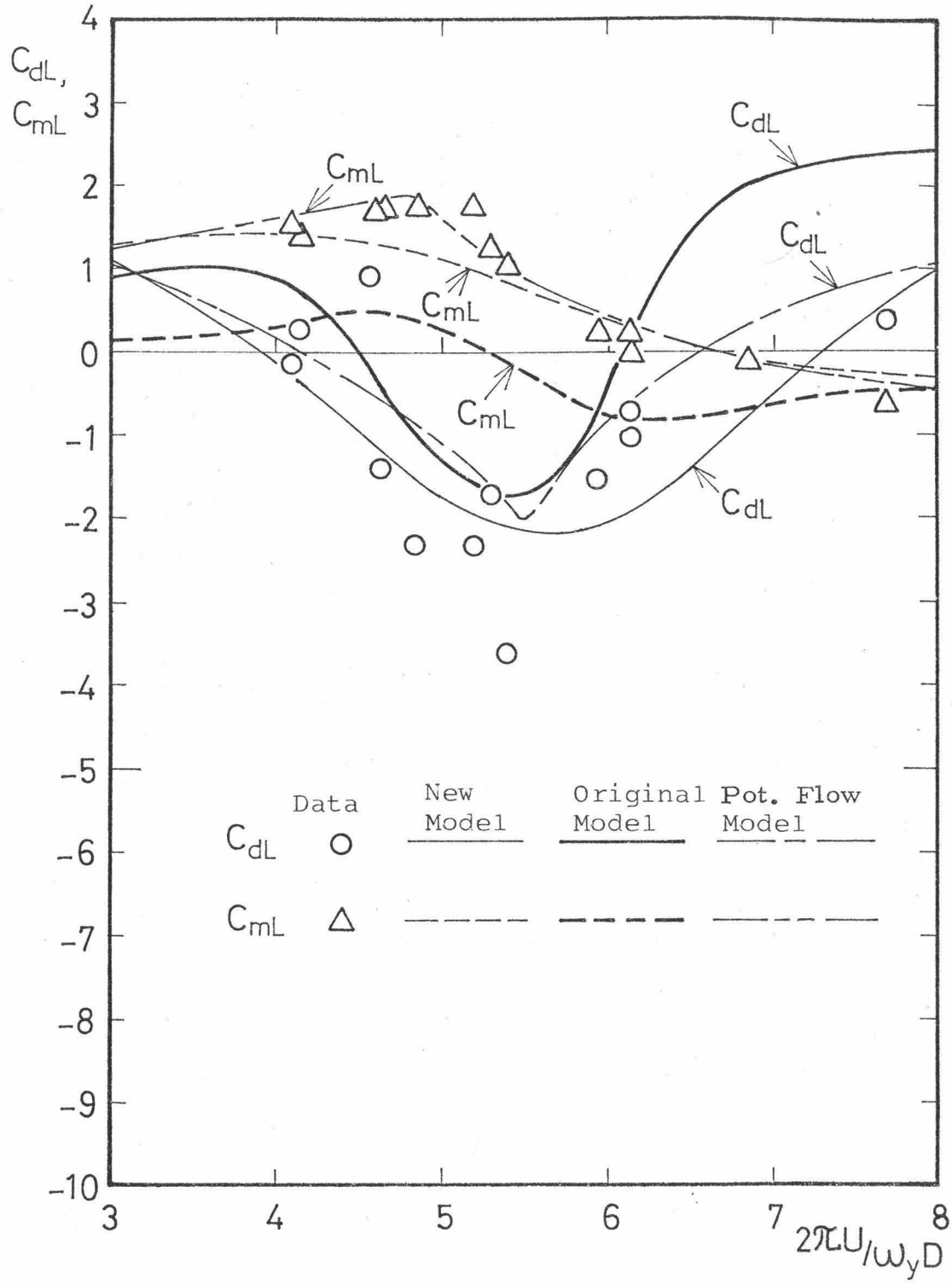

Fig. 4(b). The Lift Coefficients, C_{dL} & C_{mL}, in the Resonance Range with $A_y/D = .5$.

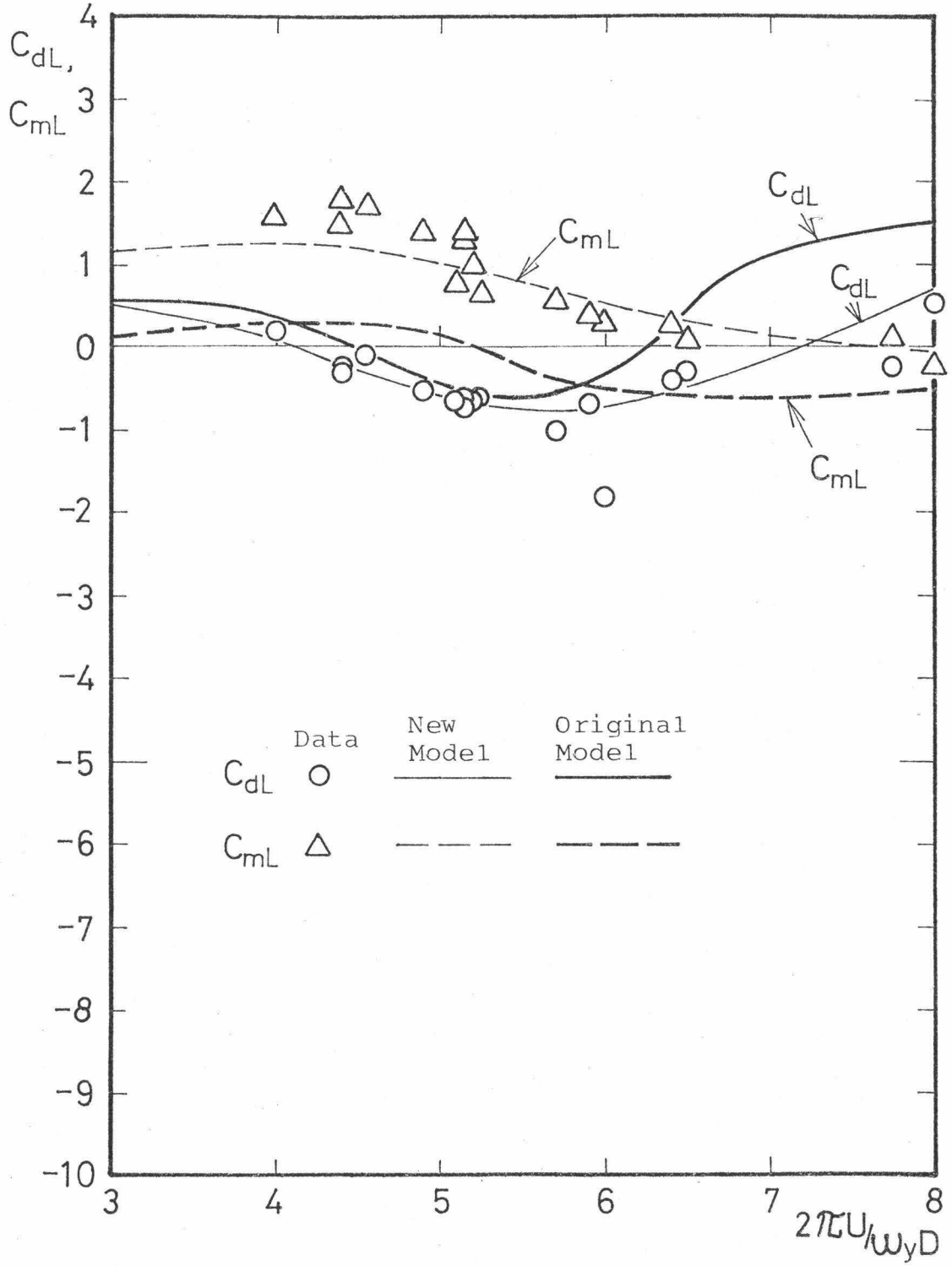

Fig. 4(c). The Lift Coefficients, C_{dL} & C_{mL}, in the Resonance Range with A_y/D = .75.

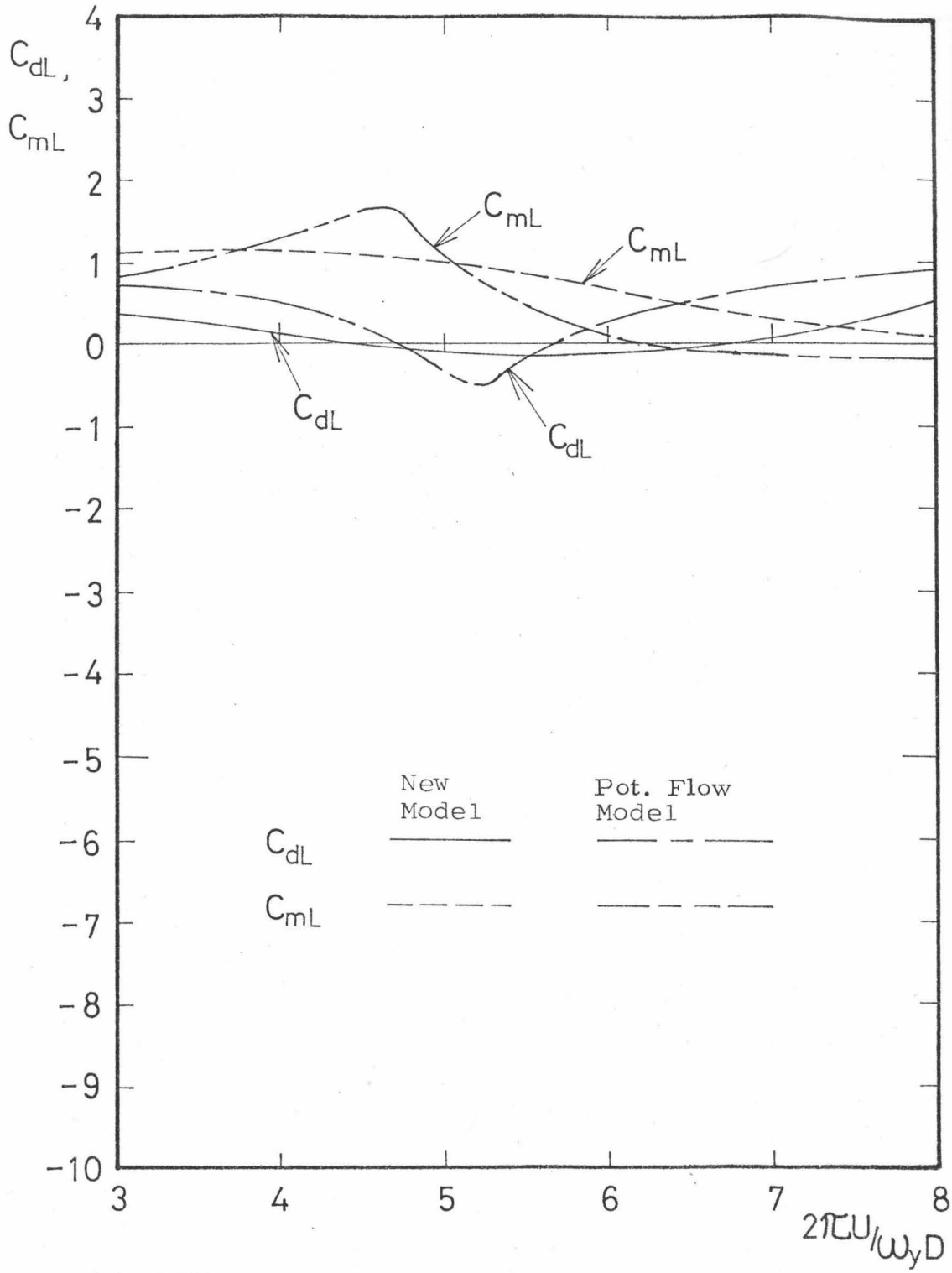

Fig. 4(d). The Lift Coefficients, C_{dL} & C_{mL}, in the Resonance Range with $A_y/D = 1.0$.

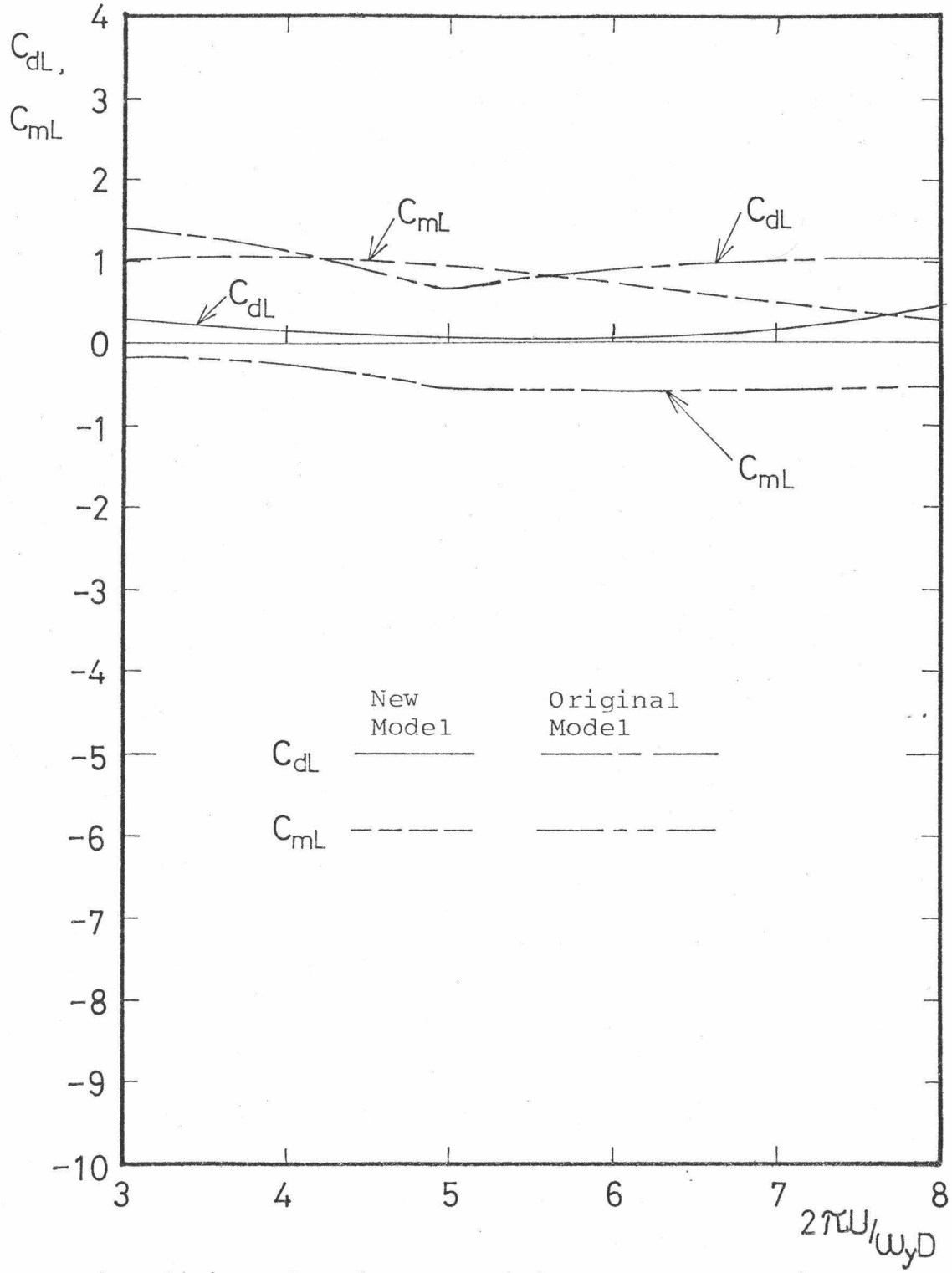

Fig. 4(e). The Lift Coefficients, C_{dL} & C_{mL}, in the Resonance Range With $A_y/D = 1.5$.

minimize the mean square difference between the analytical prediction and the data. As a starting point, the values used in the original Iwan-Blevins model [2] were assumed. The values are (using the present notation)

$$\begin{aligned} \hat{a}_0 = a_0 + a_7 &= 0.48 \\ a_1 &= 0.44 \\ a_2 &= 0 \\ a_3 &= 0.2 \\ a_4 &= 0 \\ a_5 &= 0.38 \\ a_6 &= 0 \end{aligned} \qquad (4.2.1)$$

The curves for C_{mL} and C_{dL} which result from these parameters are shown along with the data in Figs. 4(a)-4(e).

After extensive computer calculation, it was concluded that the best set of extended model parameters for the given data set are

$$\begin{aligned} \hat{a}_0 = a_0 + a_7 &= -0.346 \\ a_1 &= 0.56 \\ a_2 &= 0.18 \\ a_3 &= 0.30 \\ a_4 &= 0.68 \\ a_5 &= 0.53 \\ a_6 &= 0.78 \end{aligned} \qquad (4.2.2)$$

Curves for C_{mL} and C_{dL} which result from these parameters are also shown in Figs. 4(a)-4(e). Determination of the optimum set of

parameters is a difficult task as there are many relative minima of the mean square difference within the parameter space. However, the set of parameters given is believed to correspond closely to the absolute minimum of the mean square difference.

Figures 4(d) and 4(e) show the behavior of the extended model prediction for values of amplitude ratio $A_y/D = 1.0$ and 1.5. No experimental results for these amplitude ratios were available at the time of writing of this thesis. Also shown in Figs. 4(a)-4(e) are the smoothed results of a potential flow model study presented by Sarpkay [4].

The Strouhal number has been taken as

$$S = 0.189 \tag{4.2.3}$$

This value applies to the Reynolds number range of 5.2×10^3 to 1.16×10^4 corresponding to the experiments.

4.3 Discussion of Results

The determination of the parameters a_i has been made based on data from a forced cylinder.

The inertia and drag coefficients, C_{mL} and C_{dL}, have been defined by Eq. (4.1.1) as:

$$\frac{F_y}{0.5\rho DU^2} = C_{mL}\pi^2\left(\frac{U_m T}{D}\right)\left(\frac{D}{UT}\right)^2 \sin\theta - C_{dL}\left(\frac{U_m T}{D}\right)^2\left(\frac{D}{UT}\right)^2 |\cos\theta|\cos\theta \, . \tag{4.3.1}$$

For self sustained oscillation, the force F_y will be nearly in phase with the velocity of the cylinder. That is, C_{dL} should be negative with the absolute value of C_{dL} becoming greater as the detuning, $\Delta\omega = \omega_y - \omega_s$, approaches to zero. C_{mL}, on the other hand, arises from inertia like forces and behaves differently from C_{dL}. These facts are explicitly shown in Figs. 4(a)-(d). Figure 4(e) shows that C_{dL} does not become negative for the amplitude $A_y/D = 1.5$.

It should be emphasized that there is a special feature in the resonance region. Equation (3.2.21) gives three roots of r^2 for σ, ρ and F. The equation is

$$r^2\{(\sigma + \rho r^2)^2 + (1 - r^2)^2\} = F^2 \tag{4.3.2}$$

or

$$(1+\rho^2)r^6 - 2(1-\sigma\rho)r^4 + (\sigma^2+1)r^2 - F^2 = 0 \ . \tag{4.3.3}$$

Equation (4.3.3) is an equation of order 3 with respect to r^2. In order to solve Eq. (4.3.3) let

$$\xi \equiv r^2 - \frac{2(1-\sigma\rho)}{3(1+\rho^2)} \ , \tag{4.3.4}$$

$$p_r \equiv \frac{3(1+\rho^2)(\sigma^2+1) - 4(1-\sigma\rho)^2}{9(1+\rho^2)^2} \ , \tag{4.3.5}$$

$$q_r \equiv \frac{-16(1-\sigma\rho)^3 + 18(1+\rho^2)(1-\sigma\rho)(\sigma^2+1) - 27(1+\rho^2)^2F^2}{27(1+\rho^2)^3} \tag{4.3.6}$$

Then, Eq. (4.3.3) reduces to

$$\xi^3 + 3p_r\xi + q_r = 0 \quad . \tag{4.3.7}$$

The discriminant of this equation is given by

$$D \equiv 4p_r^3 + q_r^2 \quad . \tag{4.3.8}$$

Let

$$\left.\begin{matrix}\alpha \\ \beta\end{matrix}\right\} = \frac{-q_r \pm \sqrt{q_r^2 + 4p_r^3}}{2} \quad . \tag{4.3.9}$$

i) In the case of $D \leq 0$:

r^2 has three real roots. Let one define R and θ by

$$\alpha \equiv R e^{i\theta} \quad . \tag{4.3.10}$$

β is, then, expressed by

$$\beta = \bar{\alpha} = R e^{-i\theta} \quad . \tag{4.3.11}$$

The three real roots of ξ are

$$\left.\begin{aligned} \xi_1 &= 2\sqrt[3]{R}\ \cos\theta/3 \ , \\ \xi_2 &= 2\sqrt[3]{R}\ \cos(\theta + 2\pi)/3 \ , \\ \text{and} \\ \xi_3 &= 2\sqrt[3]{R}\ \cos(\theta + 4\pi)/3 \ . \end{aligned}\right\} \tag{4.3.12}$$

The three real roots of r^2 are then given by Eqs. (4.3.12) through (4.3.4).

ii) In the case of $D > 0$:

r^2 has one real root and two complex roots. Let one define

$$\omega = \frac{-1 + \sqrt{3}\ i}{2} \quad . \tag{4.3.13}$$

Then, the real root is

$$\xi_1 = \sqrt[3]{\alpha} + \sqrt[3]{\beta} \tag{4.3.14}$$

and the complex roots are

$$\xi_2 = \omega\sqrt[3]{\alpha} + \omega^2\sqrt[3]{\beta} \quad , \tag{4.3.15}$$

and

$$\xi_3 = \omega^2\sqrt[3]{\alpha} + \omega\sqrt[3]{\beta} \quad . \tag{4.3.16}$$

The discriminant D given by Eq. (4.3.8) is written as

$$\begin{aligned} D = \frac{1}{27(1+\rho^2)^4} \{ & 4(1+\rho^2)(\sigma^2+1)^3 - 4(1-\sigma\rho)^2(\sigma^2+1)^2 \\ & + 3(1+\rho^2)^2F^4 + 32(1-\sigma\rho)^3F^2 \\ & - 36(1+\rho^2)(1-\sigma\rho)(\sigma^2+1)F^2\} \quad . \end{aligned} \tag{4.3.17}$$

The discriminant D has been examined for $\sigma = 0$ with the parameters a_i given by Eq. (4.2.2) and it has been found that

$$\left.\begin{aligned} & D < 0 \quad \text{for } A_y/D \leq 1.013 \\ \text{and} \\ & D > 0 \quad \text{for } A_y/D \geq 1.014 \quad . \end{aligned}\right\} \tag{4.3.18}$$

In other words, r^2 has three real roots for $A_y/D \leq 1.013$ and one real root for $A_y/D \geq 1.014$, provided $\sigma = 0$ or $\omega_y = \omega_s$. There is therefore the possibility of three pairs of real roots of C_{dL} and C_{mL} for a given $2\pi U/\omega_y D$ near $\sigma = 0$. This result may explain the scattering of the datum points in Figs. 4(a)-(c).

C_{mL} and C_{dL} are given by Eqs. (4.1.11) and (4.1.12). a_4 and a_5 are given by Eqs. (4.2.2) as

$$\left.\begin{aligned} a_4 &= 0.68 \ , \\ a_5 &= 0.53 \ . \end{aligned}\right\} \tag{4.3.19}$$

Let

$$\omega_y = \omega_s(1 + \Delta\omega') \ , \tag{4.3.20}$$

where $\Delta\omega'$ is small in resonance region. Then,

$$a_5 \frac{U}{D\omega_y} = \frac{a_5}{2\pi s}(1 - \Delta\omega') = 0.446(1 - \Delta\omega') \ . \tag{4.3.21}$$

Since $\Delta\omega'$ is small, a_4 and $a_5 U/D\omega_y$ are of the same order. From Eq. (4.1.12) it may be seen that C_{dL} may have the minimum value when $\sin(\bar{\varphi} + \varphi_y) < 0$ and $\cos(\bar{\varphi} + \varphi_y) > 0$, or when $-90° < \bar{\varphi} + \varphi_y < 0°$, provided $\bar{A}/A_y$ is constant. From Eq. (4.1.11) it will be seen that C_{mL} may have the maximum value when $\cos(\bar{\varphi} + \varphi_y) > 0$ and $\sin(\bar{\varphi} + \varphi_y) > 0$, or $0° < \bar{\varphi} + \varphi_y < 90°$, provided $\bar{A}/A_y$ is a positive constant. Hence, one can understand the general behavior of $\bar{\varphi} + \varphi_y$ in Figs. 4(a)-(e) which show that $\bar{\varphi} + \varphi_y$ is first greater than $90°$ and then becomes less than $-90°$.

The third term on the right hand side of Eq. (4.1.11) may be recognized as an added mass term which just shifts the value of C_{mL} upward. That may be explained as follows. Define an added mass M_a as in the potential flow model

$$M_a = \frac{\pi}{4} \rho D^2 \tag{4.3.22}$$

then, the force arising from this added mass is given by

$$F_a = M_a \ddot{y} = -\frac{\pi}{4} \rho D^2 A_y \omega_y^2 \sin\theta \ . \tag{4.3.23}$$

The Fourier averages of the force due to the added mass yields

$$C_{mLa} \equiv \frac{2U_m T}{\pi^3 D} \int_0^{2\pi} (F_a \sin\theta) d\theta / (\rho U_m^2 D)$$

$$= 1 \tag{4.3.24}$$

and

$$C_{dLa} \equiv -\tfrac{3}{4} \int_0^{2\pi} (F_a \cos\theta) d\theta / (\rho U_m^2 D)$$

$$= 0 \ . \tag{4.3.25}$$

The third term on the right hand side of Eq. (4.1.11) is

$$\frac{4}{\pi} a_6 \ .$$

This must be equal to C_{mLa}. Therefore

$$a_6 = 0.78 \tag{4.3.26}$$

which was also given by Eq. (4.2.2) using the empirical data. Equation (4.3.25) shows that the added mass has no influence to C_{dL}.

For a free cylinder in the resonance range in which C_{dL} is negative and C_{mL} is small, the force acting on the cylinder becomes positive and in phase with the cylinder velocity. This results in the amplitude of the cylinder vibration becoming large. The velocity of the fluid expressed by $\dot{z}$ also becomes large and the out of phase $\dot{z}^3$ term becomes comparable to the $\dot{z}$ term in magnitude in the fluid oscillator equation, Eq. (3.3.1). Hence, the vibration is self-limiting. The flow oscillation in phase with the cylinder vibration yields the "locked in" phenomena associated with vortex shedding.

Figure 4(a) shows C_{mL} and C_{dL} for the amplitude of $A_y/D = 0.25$. The curves for the new model fit the data well except for $2\pi U/\omega_y D < 4$. The boundaries of the resonance region are not clear, so the curves for the new model may not fit with the data when $2\pi U/\omega_y D$ is small. The datum point of C_{dL} at $2\pi U/\omega_y D = 5.75$ is far from the curve of the new model. This may be due to the fact that there are three real roots of r^2 in this region as has been mentioned and the curves are calculated only with reference to the maximum root. It seems reasonable to take the maximum root since the vibration for this root tends to be larger than for the other roots. The curves for the potential flow model are far from the datum points. Also the curves for the original model show very poor agreement with the data.

Figure 4(b) shows another set of curves for C_{mL} and C_{dL} for $A_y/D = 0.5$. The curve for C_{mL} by the potential flow model gives the best fit with the data. That of the new model agrees fairly well with the data. The curves for C_{dL} by the potential flow model and the new model are good except for the strong resonance point at $2\pi U/\omega_y D = 5.4$.

Figure 4(c) shows C_{mL} and C_{dL} for $A_y/D = 0.75$. The new model shows good agreement with the data in both C_{mL} and C_{dL}.

Figures 4(d) and (e) give the curves of C_{mL} and C_{dL} for $A_y/D = 1.0$ and 1.5. No experimental data are available for these cases.

It is concluded that the new model shows adequate agreement with the data for all cases shown.

The values of a_i are given by Eqs. (4.2.2). Since a_0 is defined by Eq. (2.1.5) and represents the relationship between the momentum flux J_y and the transverse component of the flow within the control volume, a_0 must be positive. It is, however, reasonable that the momentum change through the control volume S_y may be influenced by the rate of the change of the transverse component of the flow, i.e., a_7 is not zero. In other words, the empirical data give a_7 negative since

$$a_7 = -a_0 - 0.346 \ . \qquad (4.3.26)$$

The parameter a_6 expresses the added mass of a cylinder as has been mentioned. It is interesting that this added mass

in a flow with vortices is essentially equal to the value in potential flow without vortices. That is a_6 appears to be nearly independent of the existence of vortices.

The parameters a_4 and a_5 represent the forces due to the relative velocity $\dot{z} - \dot{y}$ and the rate of its change $\ddot{z} - \ddot{y}$, respectively. They are positive and therefore result in forces which oppose the cylinder motion.

The parameter $a_4 - a_6$ is the coefficient of the $\ddot{y}$ term and is negative (-0.1). It plays an important role in detuning. As has been mentioned in the original model [2], the frequency entrainment of an elastically supported cylinder becomes explicit as the coefficient of the $\ddot{y}$ term ($a_4 - a_6$ in this case) becomes small. In the original model this term was taken to be zero.

All of the parameters a_1, a_2, a_3 and a_7 come from the correction terms to the momentum flux term S_y. The parameter a_7 has been mentioned. The parameters a_2 and a_3 represent nonlinear terms. When $\dot{z}$ is small, the vibration amplitude of $\dot{z}$ grows. There must therefore be negative damping in Eq. (2.1.19) or

$$a_1' - a_5' > a_3' \frac{\dot{z}^2}{U^2} \quad ; \quad \dot{z} \text{ small} \tag{4.3.27}$$

When $\dot{z}$ is large, the vibration will decay. Hence, there must be positive damping in Eq. (2.1.19) or

$$a_1' - a_5' < a_3' \frac{\dot{Z}^2}{U^2} \quad ; \quad \dot{z} \text{ large} . \tag{4.3.28}$$

Consequently, $a_1 - a_5$ and a_3 must be positive. This is also seen to be necessary in Eqs. (3.2.9), (3.2.10) and (3.2.14).

The parameter a_2 effects the naturalfrequency of the fluid oscillator. Since $a_2 > 0$, the fluid oscillator is stiffening and its effective natural frequency increases as its amplitude of oscillation increases.

CHAPTER V

CONCLUSIONS

A bluff structure exposed to a fluid flow can be excited by vortex shedding. If the frequency of vortex shedding is near the natural frequency of the structure, the vortex shedding can lock onto the structural oscillation with resulting large amplitude oscillation. The Iwan-Blevins model has been proposed to describe this fluid-structure oscillation phenomenon.

An extension of the Iwan-Blevins model has been made in this thesis. The new model is similar to the original model in that it is based on a control volume approach to the vortex shedding process and the von Karman idealization of the vortex street. The model is composed of a fluid like oscillator and a structural oscillator which interact through the force exerted between the fluid and the cylinder.

The new model has three new parameters in addition to the original model parameters. These new parameters account for a z cube type of nonlinearity in the feedback from the shed vortices to the cylinder, an unsteady force due to the change in the relative velocity between the flow and the cylinder and an additional mass. The resultant fluid oscillator is of the form of a modified Van der Pol equation. The nature of the solutions of this equation have been examined and it has been shown that the extra terms affect the amplitude and stability of the response.

The equations for an elastically mounted cylinder have been derived. The equations for the amplitude and the frequency are given in rather complex form. However, they may readily be solved numerically by iterative methods.

The model parameters are determined for a circular cylinder using the experimental data generated by Sarpkaya. A least square fit method for nonlinear functions has been used. The original and new models have been compared with data for the forced vibration of a circular cylinder. Also examined are the results of a potential flow model calculation. It is concluded that the new model shows the best agreement with the data.

Under certain conditions the amplitude of the flow oscillator may have three real roots. This fact may explain some of the scatter of the data points of C_{cL} in Figs. 4(a)-(c).

REFERENCES

1. Chen, Y.N.: Flactuating Lift Forces of the Karman Vortex Streets on Single Cylinders and in Tube Bundles: Part 1, The Vortex Street Geometry of the Single Circular Cylinder; Part 2, Lift Forces of Single Cylinders; Part 3, Lift Forces in Tube Bundles, Journal of Engineering for Industry, Transactions of the ASME, Ser. B. V.92, n. 2, pp. 603-612, 613-622, 623-628, May 1972.

2. Blevins, R.D.: Flow Induced Vibration of Bluff Structures, Ph.D. Thesis, California Institute of Technology, 1974.

3. Funakawa, M.: Vibration of Tube Banks by Wake Force, on Vibration Problems in Industry, International Symposium, Proceeding Sess. Pap., Keswick, Engl., Apr. 10-12, 1973, Sess. 4, Pap. 417, 18p.

4. Sarpkaya, T.: Notes for the 4-5 March 1976 Meeting on Cable Strumming Held at the California Institute of Technology between the Sponsors, Consultants, and the Investigators.

5. Griffin, O.M.: The Unsteady Wake of an Oscillating Cylinder at Low Reynolds Number, Journal of Applied Mechanics, Transactions of the ASME, Ser. E., V. 38, n. 4, pp. 729-738, Dec. 1971.

6. Griffin, O.M.: Flow Near Self-Excited and Forced Vibrating Circular Cylinder, Journal of Engineering for Industry, Transactions of the ASME, Ser. B, V. 94, n. 2, pp. 539-547, May 1972.

7. Iwan, W.D. and Blevins, R.D.: A Model for Vortex Induced Oscillation of Structures, Journal of Applied Mechanics, Transactions of the ASME, pp. 581-586, 1974.

8. Iwan, W.D.: The Vortex Induced Oscillation of Elastic Structural Elements, Journal of Engineering for Industry, Transactions of the ASME, pp. 1-5, 1975.

9. Blevins, R.D.: Vibration of a Loosely Held Tube, Journal of Engineering for Industry, Transactions of the ASME, pp. 1-4, 1975.

10. Minorsky, N.: Nonlinear Oscillations, Krieger Pub., 1974.

11. Stoker, J.J.: Nonlinear Vibrations, Interscience Pub., 1950.

APPENDIX

TRANSVERSE MOMENTUM

Complex potential is

$$w = -\frac{\Gamma}{2\pi_i} \log \sin \frac{\pi}{\ell}(z - z_0) + \frac{\Gamma}{2\pi_i} \log \sin \frac{\pi}{\ell}(z + z_0) + U_\infty z \quad . \tag{A-1}$$

Hence, the derivative with respect to z is

$$\frac{dw}{dz} = u - iv = -\frac{\Gamma}{2i\ell} \cot \frac{\pi}{\ell}(z - z_0) + \frac{\Gamma}{2i\ell} \cot \frac{\pi}{\ell}(z + z_0) + U_\infty \quad . \tag{A-2}$$

If $|z| \gg |z_0|$ (or $y \gg y_0$; $z = x + iy$, $z_0 = x_0 + iy_0$),

$$\frac{dw}{dz} = u - iv = U_\infty \quad , \tag{A-3}$$

or

$$\left.\begin{aligned} u &= U_\infty \quad , \\ v &= 0 \quad . \end{aligned}\right\} \tag{A-4}$$

Equation (A-1) satisfies the boundary condition. Let

$$\left.\begin{aligned} z &= x + iy \quad , \\ z_0 &= \frac{\ell}{4} + i\frac{h}{2} \quad . \end{aligned}\right\} \tag{A-5}$$

Substituting Eqs. (A-5) into Eq. (A-2) makes

$$u - iv = -\frac{\Gamma}{2i\ell} \cot \frac{\pi}{\ell}\{(x - \frac{\ell}{4}) + i(y - \frac{h}{2})\}$$

$$+ \frac{\Gamma}{2i\ell} \cot \frac{\pi}{\ell}\{(x + \frac{\ell}{4}) + i(y + \frac{h}{2})\} + U_\infty \quad . \tag{A-6}$$

Now, it is generally true that

$$\cot (x + iy) = \frac{\sin 2x - i \sinh 2y}{\cosh 2y - \cos 2x} . \tag{A-7}$$

Using Eq. (A-7), Eq. (A-6) becomes

$$u - iv = \frac{\Gamma}{2\ell} \left\{ \frac{i \sin \frac{2\pi}{\ell} (x - \frac{\ell}{4}) + \sinh \frac{2\pi}{\ell} (y - \frac{h}{2})}{\cosh \frac{2\pi}{\ell} (y - \frac{h}{2}) - \cos \frac{2\pi}{\ell} (x - \frac{\ell}{4})} \right.$$

$$\left. - \frac{i \sin \frac{2\pi}{\ell} (x + \frac{\ell}{4}) + \sinh \frac{2\pi}{\ell} (y + \frac{h}{2})}{\cosh \frac{2\pi}{\ell} (y + \frac{h}{2}) - \cos \frac{2\pi}{\ell} (x + \frac{\ell}{4})} \right\} + U_\infty . \tag{A-8}$$

Thus, the velocity components are

$$u = \frac{\Gamma}{2\ell} \left\{ \frac{\sinh \frac{2\pi}{\ell} (y - \frac{h}{2})}{\cosh \frac{2\pi}{\ell} (y - \frac{h}{2}) - \cos \frac{2\pi}{\ell} (x - \frac{\ell}{4})} \right.$$

$$\left. - \frac{\sinh \frac{2\pi}{\ell} (y + \frac{h}{2})}{\cosh \frac{2\pi}{\ell} (y + \frac{h}{2}) - \cos \frac{2\pi}{\ell} (x + \frac{\ell}{4})} \right\} + U_\infty , \tag{A-9}$$

$$v = \frac{\Gamma}{2\ell} \left\{ - \frac{\sin \frac{2\pi}{\ell} (x - \frac{\ell}{4})}{\cosh \frac{2\pi}{\ell} (y - \frac{h}{2}) - \cos \frac{2\pi}{\ell} (x - \frac{\ell}{4})} \right.$$

$$\left. + \frac{\sin \frac{2\pi}{\ell} (x - \frac{\ell}{4})}{\cosh \frac{2\pi}{\ell} (y + \frac{h}{2}) - \cos \frac{2\pi}{\ell} (x + \frac{\ell}{4})} \right\} . \tag{A-10}$$

Similar to Chen's model [3], let

$$x = k\ell \ , \qquad k = 0, 1, 2, \ldots \ .$$

Then, Eqs. (A-9) and (A-10) reduce to

$$u = \frac{\Gamma}{2\ell} \left\{ \tanh \frac{2\pi}{\ell} \left(y - \frac{h}{2}\right) - \tanh \frac{2\pi}{\ell} \left(y + \frac{h}{2}\right) \right\} + U_\infty \ , \qquad \text{(A-11)}$$

$$v = \frac{\Gamma}{2\ell} \left\{ \frac{1}{\cosh \frac{2\pi}{\ell} \left(y - \frac{h}{2}\right)} + \frac{1}{\cosh \frac{2\pi}{\ell} \left(y + \frac{h}{2}\right)} \right\} \ . \qquad \text{(A-12)}$$

The momentum along to y-axis is

$$S_y = \int_{-\infty}^{\infty} \rho uv dy \ . \qquad \text{(A-13)}$$

From Eqs. (A-11) and (A-12), we get

$$uv = \left(\frac{\Gamma}{2\ell}\right)^2 \left\{ \frac{\sinh \frac{2\pi}{\ell} \left(y - \frac{h}{2}\right)}{\cosh^2 \frac{2\pi}{\ell} \left(y - \frac{h}{2}\right)} - \frac{\sinh \frac{2\pi}{\ell} \left(y + \frac{h}{2}\right)}{\cosh^2 \frac{2\pi}{\ell} \left(y + \frac{h}{2}\right)} \right.$$

$$\left. + \frac{\tanh \frac{2\pi}{\ell} \left(y - \frac{h}{2}\right)}{\cosh \frac{2\pi}{\ell} \left(y + \frac{h}{2}\right)} - \frac{\tanh \frac{2\pi}{\ell} \left(y + \frac{h}{2}\right)}{\cosh \frac{2\pi}{\ell} \left(y - \frac{h}{2}\right)} \right\}$$

$$+ \frac{\Gamma U_\infty}{2\ell} \left\{ \frac{1}{\cosh \frac{2\pi}{\ell} \left(y - \frac{h}{2}\right)} + \frac{1}{\cosh \frac{2\pi}{\ell} \left(y + \frac{h}{2}\right)} \right\} \ . \qquad \text{(A-14)}$$

Now, it is generally true that

$$I[1,-2] = \int_{-\infty}^{\infty} \sinh x \cosh^{-2} x\,dx$$

$$= \left[\sinh^2 x \cosh^{-1} x + \frac{1-2+2}{-1} I[1,0] \right]_{-\infty}^{\infty}$$

$$= [\sinh^2 x \cosh^{-1} x - \cosh x]_{-\infty}^{\infty}$$

$$= [-\cosh^{-1} x]_{-\infty}^{\infty}$$

$$= 0 \quad . \qquad \text{(A-15)}$$

$$\int_{-\infty}^{\infty} \frac{\tanh \frac{2\pi}{\ell}(y - \frac{h}{2})}{\cosh \frac{2\pi}{\ell}(y + \frac{h}{2})} - \frac{\tanh \frac{2\pi}{\ell}(y + \frac{h}{2})}{\cosh \frac{2\pi}{\ell}(y - \frac{h}{2})}\, dy$$

$$= \int_{-\infty}^{\infty} \frac{\sinh \frac{2\pi}{\ell}(y - \frac{h}{2}) - \sinh \frac{2\pi}{\ell}(y + \frac{h}{2})}{\cosh \frac{2\pi}{\ell}(y + \frac{h}{2}) \cosh \frac{2\pi}{\ell}(y - \frac{h}{2})}\, dy$$

$$= - \int_{-\infty}^{\infty} \frac{4 \cosh \frac{2\pi}{\ell} y \sinh \frac{\pi h}{\ell}}{\cosh \frac{2\pi}{\ell} 27 + \cosh \frac{2\pi}{\ell} h}\, dy$$

$$= -2 \sinh \frac{\pi}{\ell} h \int_{-\infty}^{\infty} \frac{\cosh \frac{2\pi}{\ell} y}{\cosh^2 \frac{2\pi}{\ell} y + \cosh^2 \frac{\pi h}{\ell} - 1}\, dy$$

$$= -2 \sinh \frac{\pi}{\ell} h \int_{-\infty}^{\infty} \frac{\cosh \frac{2\pi}{\ell} y}{\sinh^2 \frac{2\pi}{\ell} y + \cosh^2 \frac{\pi h}{\ell}}\, dy$$

-continued-

$$= -\frac{\ell}{\pi}\tanh\frac{\pi}{\ell}h \int_{-\infty}^{\infty} \frac{\frac{2\pi}{\ell}\frac{\cosh\frac{2\pi}{\ell}y}{\cosh\frac{\pi h}{\ell}}}{1+\left(\frac{\sinh\frac{2\pi}{\ell}y}{\cosh\frac{\pi h}{\ell}}\right)^2}\,dy$$

$$= -\frac{\ell}{\pi}\tanh\frac{\pi}{\ell}h\left[\arctan\left(\frac{\sinh\frac{2\pi}{\ell}y}{\cosh\frac{\pi h}{\ell}}\right)\right]_{-\infty}^{\infty}$$

$$= -\ell\tanh\frac{\pi}{\ell}h \quad . \tag{A-16}$$

$$\int_{-\infty}^{\infty} \operatorname{sech}\frac{2\pi}{\ell}(y\pm\frac{h}{2})dy = \frac{\ell}{2\pi}\left[\arctan\{\sinh\frac{2\pi}{\ell}(y\pm\frac{h}{2})\}\right]_{-\infty}^{\infty}$$

$$= \frac{\ell}{2\pi}\left[\frac{\pi}{2}+\frac{\pi}{2}\right] = \frac{\ell}{2} \quad . \tag{A-17}$$

Using Eqs. (A-14) - (A-17), Eq. (A-13) becomes

$$S_y = -\rho\left(\frac{\Gamma}{2\ell}\right)^2\cdot\ell\tanh\frac{\pi}{\ell}h + \rho\frac{\Gamma U_\infty}{2\ell}\cdot\ell$$

$$= \tfrac{1}{2}\rho\Gamma(U_\infty - \frac{\Gamma}{2\ell}\tanh\frac{\pi}{\ell}h)$$

$$= \tfrac{1}{2}\rho\Gamma(U_\infty - u_t) \quad , \tag{A-18}$$

where u_t is the translational velocity of vortices in stational fluid and

$$u_t = \frac{\Gamma}{2\ell}\tanh\frac{\pi}{\ell}h \quad . \tag{A-19}$$

Note: The translational velocity is given as follows:

$$w = \left[-\frac{\Gamma}{2\pi_i} \log \sin \frac{\pi}{\ell}(z - z_0) + \frac{\Gamma}{2\pi_i} \log \sin \frac{\pi}{\ell}(z + z_0) + \frac{\Gamma}{2\pi_i} \log (z - z_0) \right]_{z=z_0}$$

$$\frac{dw}{dz} = u_0 - iv_0 = \left[-\frac{\Gamma}{2i\ell} \cot \frac{\pi}{\ell}(z-z_0) + \frac{\Gamma}{2i\ell} \cot \frac{\pi}{\ell}(z+z_0) + \frac{\Gamma}{2\pi_i} \frac{1}{z-z_0} \right]_{z=z_0}$$

$$= \frac{\Gamma}{2\ell} \left[\frac{1}{i} \cot \frac{\pi}{\ell}(z+z_0) - \frac{\ell/\pi}{i(z-z_0)} \left\{ \frac{\pi}{\ell}(z-z_0) \cot \frac{\pi}{\ell}(z-z_0) - 1 \right\} \right]_{z=z_0}$$

$$= \frac{\Gamma}{2\ell} \left[\frac{1}{i} \cot \frac{\pi}{\ell}(z+z_0) - \frac{\ell/\pi}{i(z-z_0)} \left\{ \frac{\ell^2}{3\pi^2}(z-z_0)^2 + \frac{\ell^4}{45\pi^4}(z-z_0)^4 + \cdots \right\} \right]_{z=z_0}$$

$$= \frac{\Gamma}{2i\ell} \cot \frac{2\pi}{\ell} z_0 = \frac{\Gamma}{2i\ell} \cot \frac{2\pi}{\ell} \left(\frac{\ell}{4} + i \frac{h}{2} \right)$$

$$= \frac{\Gamma}{2\ell i} \frac{1 - i \tan \frac{2\pi}{\ell} \frac{\ell}{4} \tanh \frac{2\pi}{\ell} \frac{h}{2}}{\tan \frac{2\pi}{\ell} \frac{\ell}{4} + i \tanh \frac{2\pi}{\ell} \frac{h}{2}}$$

$$= -\frac{\Gamma}{2\ell} \tanh \frac{\pi h}{\ell}$$

Then

$$u_t = |u_0| = \frac{\Gamma}{2\ell} \tanh \frac{\pi h}{\ell} \qquad \text{(A-20)}$$

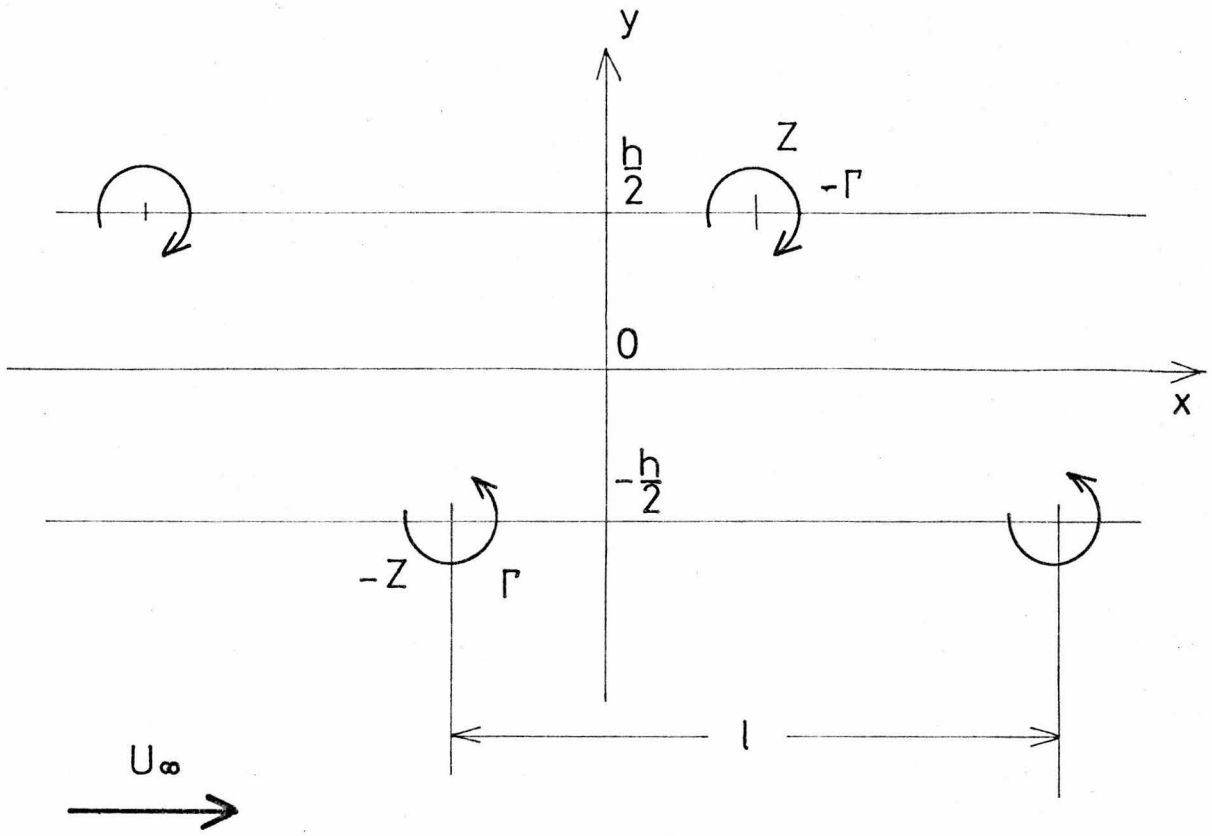

Z - plane

Fig. A-1. Karman Vortex Street.